

# On Using Classification Datasets to Evaluate Graph Outlier Detection: Peculiar Observations and New Insights

LINGXIAO ZHAO, Heinz College - Information Systems & Public Policy, Carnegie Mellon University, USA  
 LEMAN AKOGLU, Heinz College - Information Systems & Public Policy, Carnegie Mellon University, USA

It is common practice of the outlier mining community to repurpose classification datasets toward evaluating various detection models. To that end, often a binary classification dataset is used, where samples from (typically, the larger) one of the classes is designated as the ‘inlier’ samples, and the other class is substantially down-sampled to create the (ground-truth) ‘outlier’ samples. In this study, we identify an intriguing issue with repurposing graph classification datasets for graph outlier detection in this manner. Surprisingly, *the detection performance of outlier models depends significantly on which class is down-sampled*; put differently, accuracy often “flips” from high to low depending on which of the classes is down-sampled to represent the outlier samples. The problem is notably exacerbated particularly for a certain family of *propagation based* outlier detection models. Through careful analysis, we show that this issue mainly stems from disparate within-class sample similarity – which is amplified by various propagation based models – that impacts key characteristics of inlier/outlier distributions and indirectly, the difficulty of the outlier detection task and hence performance outcomes. With this study, we aim to draw attention to this (to our knowledge) previously-unnoticed issue, as it has implications for fair and effective evaluation of detection models, and hope that it will motivate the design of better evaluation benchmarks for outlier detection. Finally, we discuss the possibly overarching implications of using propagation based models on datasets with disparate within-class sample similarity beyond outlier detection, specifically for graph classification and graph-level clustering tasks.

## 1 INTRODUCTION

Outlier detection is a critical task that finds numerous applications in healthcare, security, finance, etc. [1]. Simply put, the task is to identify observations that notably stand out within large collections of data so as to “arouse suspicions that [they were] generated by a different mechanism” [11]. One of the key challenges of outlier detection is that it poses an *unsupervised* learning problem. Due to the rare nature of outlier instances, combined with the laborious manual (i.e., human) labeling, access to benchmark datasets with sufficiently many labeled ground-truth outliers is limited.

**Motivation.** Lack of labeled benchmark datasets for outlier detection is not only a challenge for learning, but also for the *evaluation* of outlier models. Even if one designs unsupervised models for the detection task, ground-truth labels that truly reflect the nature of outliers in a domain is essential for the reliable error estimation of various models. Thereby, the scarcity of representative labeled outliers in real-world datasets has motivated a couple of strategies for building benchmark datasets, mainly for evaluation.

One strategy is to inject realistic yet synthetic outliers into real-world datasets via simulation. For example, in fraud detection applications, one could simulate activities that reflect malicious schemes known to domain experts in order to obtain positive (i.e., anomalous) observations. Emmott *et al.* [6, 7] present a systematic in-depth study on this subject. This approach is typically criticized for

---

Authors’ addresses: Lingxiao Zhao, lingxia1@andrew.cmu.edu, Heinz College - Information Systems & Public Policy, Carnegie Mellon University, 5000 Forbes Ave, Pittsburgh, PA, USA, 15213; Leman Akoglu, lakoglu@andrew.cmu.edu, Heinz College - Information Systems & Public Policy, Carnegie Mellon University, 5000 Forbes Ave, Pittsburgh, PA, USA, 15213.

---

Permission to make digital or hard copies of part or all of this work for personal or classroom use is granted without fee provided that copies are not made or distributed for profit or commercial advantage and that copies bear this notice and the full citation on the first page. Copyrights for third-party components of this work must be honored. For all other uses, contact the owner/author(s).

© 2021 Copyright held by the owner/author(s).

a couple of reasons. First, the simulated outliers are limited to the known anomalous behaviors and may not comprehensively reflect the outliers in the wild. Second, this type of approach may create an environment fertile to “leakage”, where the outliers may be simulated in a biased way that aligns with how the detection model under evaluation works.

An alternative strategy to artificial outlier injection is to repurpose classification datasets so as to work with only real-world samples. (See [3] and citations therein.) A common practice is to use binary classification datasets, where samples from one of the classes (typically the one with the larger number of samples) is treated as the ‘inlier’ samples, and the other class is down-sampled (to a desired rate) to constitute the ‘outlier’ samples. This procedure conforms with the notion of outlierness as characterized by Hawkins [11], in that the outliers are drawn from a data distribution (i.e., class) that is different from that generating the inliers. In their in-depth evaluation of unsupervised outlier detection models, Campos *et al.* [3] mainly adopt this strategy.

**This paper.** In this study we scrutinize this latter strategy, and pose the following questions: *Should one use classification datasets for evaluating outlier detection models? What issues should one be aware of in designing benchmark datasets in this manner?* Specifically, we study this issue in the context of outlier detection in *graph databases*, where given a collection of graphs, the task is to identify the outlier graphs that stand out. In many settings, one of the classes has a natural semantic affinity to being ‘outlier’; for example, ‘sick’ patients with a certain disease (vs. healthy patients), tweets pertaining to ‘hate speech/bullying/fake news/etc.’ (vs. regular tweets). In others, the choice of which class to down-sample is arbitrary. The peculiar issue that we identify is exactly about this arbitrary choice: **We observe that the detection performances of outlier models depend significantly on which class is down-sampled.**

Before delving into details, we start by illustrating this intriguing issue empirically. Table 1 (See Sec. 3.1) shows the ROC-AUC performances of three graph embedding based outlier detectors based on four binary graph classification datasets. Each dataset has two variants, each corresponding to one of the classes down-sampled as outlier. The difference in performances between the two variants is striking, consistently across models on most (although not all) datasets.

**Related work.** To the best of our knowledge, this issue has not been raised previously by any prior work on outlier detection. Campos *et al.* [3] state that “random downsampling often leads to great variation in the nature of the outliers produced” and that “observations based on downsampling can vary considerably from sample to sample”, based on which they repeat their down-sampling procedure 10 times per dataset “to mitigate the impact of randomization”. This, however, points to an orthogonal issue as it pertains to down-sampling *after* deciding (i.e. fixing) *which* class to down-sample. Repurposing classification datasets for evaluation of clustering has been questioned by Färber *et al.* [8], which alludes to the potential misalignment between the semantics of data clusters and class labels. Our study points to an issue orthogonal to semantics.

**Contributions.** Through extensive analysis, our study aims to (1) illustrate the issues with using graph classification datasets for creating outlier benchmarks for model evaluation, (2) identify the leading factors behind these issues, (3) propose concrete measures to quantify these factors and explain their possible driving mechanisms, and last but not the least (4) build and publicly share a Deep Graph-Level Anomaly Detection library called DeepGLAD, along with all the datasets used in our study, to enable the community to use in their “GLAD” tasks and also to facilitate further investigation into the issues raised through our study. We outline the main contributions of this work as follows.

- **Study of Deep Graph-level Outlier Detection:** We start with the design and evaluation of two different categories of models for outlier detection in graph databases; namely, (1) two-stage models—pipelining unsupervised graph-level representation learning with off-the-shelf

point-cloud outlier detectors, and (2) end-to-end models—learning representations simultaneously with optimizing an anomaly detection objective, such as one-class classification or reconstruction loss. (Sec. 2)

- **“Performance Flip” Issue with Using Classification Datasets for Evaluation:** To evaluate the aforementioned graph outlier models, we construct labeled benchmark datasets by repurposing binary graph classification datasets. Notably, we down-sample those datasets in *both* “directions”, that is, we create *two* benchmark variants *per* classification dataset, respectively down-sampling one or the other class samples to constitute the outlier graphs. Surprisingly, we find that most models, while achieving high detection performance on one variant, fail considerably on the other. That is, we identify the intriguing issue of what we call “performance flip” depending on which class has been down-sampled. (Sec. 3.1)
- **Driving Factors behind “Performance Flip”:** Roughly put, we find that the issue stems from the (mis)alignment between the inlier/outlier distributions created by graph embedding techniques and key underlying assumptions of the detection models. While one scenario creates a dense inlier distribution surrounded with dispersed outliers (‘easy’ task), the other creates a sparse inlier distribution that has overlapping support with a small set of outliers with relatively higher density (‘hard’ task). Since most models assume the former scenario in their formalism, they ‘do well’ on the respective ‘easy’ task.

We identify two key leading factors behind the observed “performance flip” issue, particularly (1) *density disparity*; where the density of graph embeddings differ considerably between two classes, and (2) *overlapping support*; where the distributions of graph embeddings from the two classes exhibit overlapping support in the representation space. Moreover, we point out two contributing factors: (a) initial disparity between within-class sample similarities, and (b) amplification of this disparity by graph propagation – called *sparsification* – which is a property of some graph embedding models (Sec 3.2). We design quantitative metrics to concretely measure those factors (Sec. 3.3), and analyze the sparsification property via controlled simulations on  $k$ -regular graphs (Sec. 3.4). Finally, we present a detailed empirical study on four real-world datasets (Sec. 4).

- **Insights for Outlier Detection and Beyond:** Our findings have implications for the fair and systematic evaluation of outlier models. Specifically, our study puts the spotlight onto thinking about task difficulty as well as the alignment between the underlying data manifolds and model assumptions, in designing evaluation benchmarks for outlier detection. Moreover, we argue that issues we identify may extend beyond outlier detection, with possible implications on graph classification and clustering.

We point out that almost all GNN models employ a message-passing based propagation mechanism, as such, they also have the potential of suffering from sparsification. Specifically, this can cause severe overfitting for graph classification when the number of labeled samples is small. It can also adversely affect graph-level clustering tasks that aim to identify dense regions in the (representation) space. (Sec. 5)

- **Open-source DeepGLAD Library<sup>1</sup> and Datasets:** To facilitate further investigation on these and related issues, we open-source our DeepGLAD library (containing 10+ graph outlier models) as well as all the datasets we used in this study.

---

<sup>1</sup>DeepGLAD Library for graph-level anomaly detection via graph embedding: <https://tinyurl.com/deepglad>

## 2 ESSENTIAL BACKGROUND: OUTLIER DETECTION PROBLEM & MODELS

In this paper we focus on the graph-level outlier detection problem. The intriguing “performance flip” issue we observe arises from repurposing binary graph classification datasets for outlier detection evaluation. As far as we know, there is limited work studying the graph-level outlier detection problem, where the goal is to discover graphs with rare, unusual patterns which can be distinguished from the majority of graphs in a database. We call attention to the problem as it applies to many important real-world tasks from diverse domains such as drug discovery, money laundering, molecular synthesis, rare human pose detection [19], fake news detection [20], traffic events detection [10], and buggy software detection [16].

In this section we first define the problem setting followed by three different detection methods we have used to address the problem. We make several peculiar observations, as discussed in the next section, consistently across models on many (although not all) datasets.

### 2.1 Graph-Level Outlier Detection

Let  $G = (\mathcal{V}, \mathcal{E}, \mathbf{X})$  be an attributed or labeled graph with  $\mathcal{V}$  and  $\mathcal{E}$  depicting its vertex set and edge set, where each node  $i \in \mathcal{V}$  is associated with a feature vector  $\mathbf{x}_i \in \mathbb{R}^d$  and  $\mathbf{X} = [\mathbf{x}_1, \dots, \mathbf{x}_n]^T$  denotes the feature matrix,  $n = |\mathcal{V}|$  being the total number of nodes. For labeled graphs, each node feature vector  $\mathbf{x}_i \in \mathbb{R}^d$  is a one-hot encoded vector with  $d$  being the total number of unique (discrete) node labels.

**Definition 2.1** (Graph-Level Outlier Detection Problem). Given a graph database  $\mathcal{G} = \{G_1, \dots, G_N\}$  containing  $N$  labeled or attributed graphs, find the graphs that differ significantly from the majority of graphs in  $\mathcal{G}$ .

The above problem is a general statement for graph-level outlier detection. In the real-world how one defines rareness or the degree of difference to the majority may be critical and may change depending on the application. Under the setting where one repurposes binary graph classification datasets by down-sampling graphs from one class to be designated as ground-truth outliers, the problem becomes accurately flagging those down-sampled graphs from the database.

### 2.2 Graph-level Outlier Detection Models

As the graph-level outlier detection is rarely studied, there does not exist specifically designed methods for it, especially for labeled or attributed graphs. On the other hand, several existing methods for solving graph classification can be easily modified for tackling the problem. In this paper we mainly focus on three methods that can be categorized as two types: two-stage versus end-to-end. For the purposes of this paper, we find these three methods to be sufficiently illustrative of the issues we discover. It is noteworthy that they provide a framework based on which a larger list of methods can be designed, which we aim to release as part of our DeepGLAD library.

**2.2.1 Two-Stage Graph Outlier Detection.** Two-stage graph outlier detection approaches first transform graphs into graph embeddings or similarities between graphs by using unsupervised graph embedding methods (such as graph2vec [23] and FGSD [32]) or graph kernels (such as feiler-Leman kernel [31] and propagation kernel [25]). Then traditional outlier detectors such as Isolation Forest [17], Local Outlier Factor (LOF [2]), and one-class SVM (OCSVM) [18] can be used to detect outliers in the embedding (vector) space. These approaches are easy to use and do not require much hyperparameter tuning, which makes them relatively stable for an unsupervised task like outlier detection. Nevertheless, two-stage methods may suffer from suboptimal solution as the feature extractor and outlier detector are independent. Moreover, most unsupervised graph feature

extractors produce “hand-crafted” features that are deterministic without much room to improve, which further restrict the capacity of two-stage methods.

To illustrate the performance flip issue, we focus on graph kernel based two-stage approaches with two well-known outlier detectors used downstream: OCSVM and LOF. A graph kernel defines a kernel function  $\mathcal{K}$  that outputs a similarity between two graphs. Formally it can be written as

$$\mathcal{K}(G, G') = \langle \phi(G), \phi(G') \rangle_{\mathcal{H}} \quad (1)$$

where  $\mathcal{H}$  is a RKHS and  $\langle \cdot, \cdot \rangle$  is the dot product in  $\mathcal{H}$ . The mapping  $\phi(G)$  transforms graph  $G$  to an embedding vector in  $\mathcal{H}$ , which in our case contains counts of atomic subgraph patterns. Specifically we use the Weisfeiler-Leman subtree kernel and the propagation kernel, described as follows.

**Weisfeiler-Leman Subtree Kernel.** Inspired by Weisfeiler-Leman (WL) test of graph isomorphism [34] (a.k.a. the color-refinement algorithm), WL subtree kernel [31] processes a labeled graph by iteratively re-labeling each vertex with a new label compressed from a multiset label consisting of the vertex’s original label and the sorted labels of its neighbors. This procedure repeats for  $L$  iterations for all graphs and outputs  $L$  re-labeled graphs  $\{G_1, \dots, G_L\}$  for every graph  $G$ . One can easily show that each vertex in  $G_l$  at  $l$  iterations represents the subtree of the original vertex with depth  $l$ . WL subtree kernel compares two graphs by simply counting the number of co-occurrences of labels in both graphs at each iteration. The similarity score of two graphs is the summation of similarities across iterations. Formally, one can write it as

$$\mathcal{K}_{WL}(G, G') = \sum_{l=0}^L \langle \phi_{WL}(G_l), \phi_{WL}(G'_l) \rangle \quad (2)$$

where  $G_0$  represents the original input graph, and  $\phi_{WL}$  counts the frequency of all labels in the input graph by a vector with length equal to the number of unique labels.

**Sparsification.** Next we highlight a key property of the WL subtree kernel that is closely related to the performance flip issue we discover. Substructure-based graph kernels consider each substructure as a separate feature to compare among graphs. The total number of distinct substructures grows exponentially in the diameter of the substructures, which leads to the *sparsity problem* – that only a limited number of substructures would be shared among graphs. This property has also been referred to as *diagonal dominance* [22, 36] – wherein each individual graph would mostly be similar only to itself but not much to any other graph. Being based on substructures, WL subtree kernel distinguishes each  $k$ -hop subgraph as a separate feature (re-labeled as a different label), as such, its feature space tends to grow exponentially in the number of iterations. The sparsification property of WL kernel is visualized in Fig. 1, where the diagonal dominance and diminishing similarity among graphs are observed clearly.

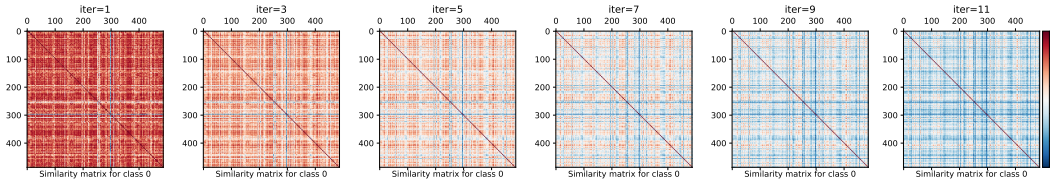


Fig. 1. Sparsification in WL subtree kernel: Pairwise similarity of graphs (from DD dataset) decreases with increasing number of iterations (left to right).

**Propagation Kernel.** Propagation kernel (PK) [25] is inspired from the idea of propagating label information among nodes over the graph structure such as label propagation algorithm [38] for

semi-supervised node classification and can be used for both attributed graphs and one-hot encoded labeled graphs. For each graph  $G = (\mathcal{V}, \mathcal{E}, X)$ , let  $X_0 = X$  denote the original feature matrix. Then PK generates a new feature matrix at each iteration by propagating the feature matrix using the transition matrix  $T = D^{-1}A$  (where  $A$  is the adjacency matrix and  $D$  is the diagonal degree matrix) of the graph. Formally,  $X_{l+1} = TX_l$ . Similar to WL subtree kernel, PK compares two graphs at each iteration. The similarity between two graphs is measured based on propagated features through binning. Formally we can write the kernel as

$$\mathcal{K}_{PK}(G, G') = \sum_{l=0}^L \langle \phi_{PK}(X_l^G), \phi_{PK}(X_l^{G'}) \rangle \quad (3)$$

where  $\phi_{PK}(\cdot)$  denotes the hash function that maps a given set of (feature) vectors into bins. To preserve locality and keep efficiency, locally sensitive hashing (LSH) [9] is used for the binning.

**Sparsification.** The propagation kernel also exhibits the aforementioned sparsity problem, increasingly for larger number of iterations. Compared to WL subtree kernel that generates new features via re-labeling (a hard transformation), propagation kernel generates new features via multiplying by the transition matrix (a soft transformation). As such, the feature space grows much slower for PK. As illustrated in Fig. 2, the diagonal dominance still holds while the sparsification occurs at a lower rate than WL subtree kernel (cf. Fig. 1).

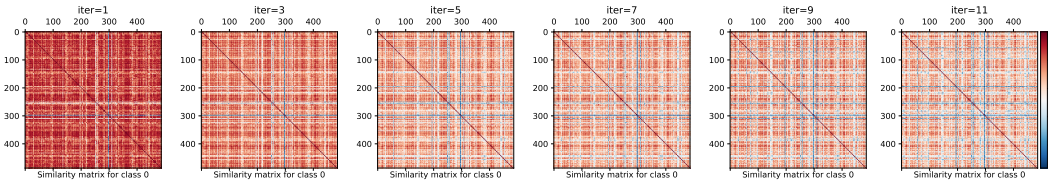


Fig. 2. Sparsification in PK: Pairwise similarity of graphs (from DD dataset) decreases with increasing number of iterations (left to right).

**2.2.2 End-to-End Deep Graph Outlier Detection.** Deep learning methods have been used for outlier detection recently to enhance automatic feature learning for high-dimensional and structured data such as images. Recently graph neural network (GNN) has achieved great success in graph-structured data, and several works have successfully applied GNNs to node-level outlier detection on a single graph, such as OCGNN [33] and DOMINANT [5]. However there is no deep model proposed for graph-level outlier detection.

Here we present a GNN model adapted from graph classification, and leverage a one-class classification objective function to address graph-level outlier detection. Compared with the widely used Graph Convolution Network (GCN) [14] model, Graph Isomorphism Network (GIN) [35] has been shown to be as powerful as the WL test of graph isomorphism, as such, we design a GIN based graph-level outlier detector. Note that an earlier GNN model called DGCNN [37] has discussed its connection to WL subtree kernel and propagation kernel. GIN builds on the ideas of DGCNN, and as a result also shares connection to these graph kernels. As we will present the issues we have discovered based on those graph kernels, we have also empirically verified that similar issues are observed for the GIN based model. In the following, we present our GIN based graph-level outlier detector, which is trained end-to-end through one-class classification loss.

Let  $h_v^{(l)}$  be the  $l$ -th layer representation of node  $v$  in the GIN model. GIN updates node representations at each layer by

$$h_v^{(l)} = \text{MLP}^{(l)}\left((1 + \epsilon^{(l)}) \cdot h_v^{(l-1)} + \sum_{u \in \mathcal{N}(v)} h_u^{(l-1)}\right) \quad (4)$$

where MLP denotes a multi-layer perceptron (we use 2 layer) and  $\mathcal{N}(v)$  denotes the direct neighbors of node  $v$ . Note that the summation operation around neighbor vectors can cause numerical explosion over iterations, thus batch normalization is applied between each GIN layer to prevent it.

After  $L$  layers, GIN generates the graph-level representation (i.e. graph embedding) using a readout function as follows.

$$h_G = \text{CONCAT}\left(\text{READOUT}(\{h_v^{(l)} | v \in G\}) \mid l = 0, 1, \dots, L\right). \quad (5)$$

While the original paper [35] proposed summation for the READOUT function to preserve maximum capacity, we use averaging (i.e. mean pooling) to account for different graph sizes in the database.

To build one-class classification into the GIN model, we borrow the idea from DeepSVDD [30]. Specifically, we optimize the one-class deep SVDD objective at the output layer of the GIN model as

$$\min_W \frac{1}{N} \sum_{i=1}^N \|\text{GIN}(G_i; W) - c\|^2 + \frac{\lambda}{2} \sum_{l=1}^L \|W^l\|_F^2 \quad (6)$$

where  $W^l$  denotes the parameter of GIN at the  $l$ -th layer,  $W = \{W^1, \dots, W^L\}$ , and  $c$  is the center of the hypersphere in the representation space that is obtained as the average of all graph representations upon initializing GIN model. Note that the second term corresponds to weight decay of deep models. As mentioned in [30], deep one-class classification suffers from feature collapse, where the trained model maps all input instances to the (constant)  $c$ . We employ the regularizations proposed therein to prevent this problem. After training the model on all graphs, the distance to center is used as the outlier score for each graph.

### 3 USING CLASSIFICATION DATASETS FOR OUTLIER MODEL EVALUATION: ISSUES

In this section we present in more detail the peculiar “performance flip” issue and related observations – associated with repurposing graph classification datasets for evaluating graph outlier detection models as presented in the previous section. Before delving into details, we outline how we discovered those issues and why we think they are important.

Motivated by the recent success of CNN-based deep models for image outlier detection, we have designed deep detection models for graph outlier detection, with the goal of leveraging the representation power of graph neural networks (GNNs). We created a testbed for evaluating the performance of a number of GNN model variants that we designed using several different binary classification datasets – per which we created two versions; by down-sampling one class or the other. We observed the peculiar performance flip issue for almost all GNN models on most (yet not all) of the datasets.

Having a clear understanding of this issue becomes critical for effectively and fairly evaluating detection models and consequently, being able to design better detectors. To that end, we investigate the potential driving factors behind the performance flip (and related) observations through empirical analysis. While the observations hold across all three models we considered (Sec. 2), they are easier to explain for the propagation based graph kernel methods relative to GNN based models. The former follow deterministic procedures whereas the latter are much more complex, involving parameter training. In the context of graph classification, Zhang *et al.* [37] argued that there is a close connection between propagation based graph kernels and GNN models. Therefore,

we believe the underlying driving mechanisms are similar, although a theoretical analysis is needed to ascertain the connection and fully understand the effects behind our observations.

In the following, we present the peculiar observations in detail (Sec. 3.1), state our hypothesis on the driving mechanisms behind these observations (Sec. 3.2), and introduce qualitative and quantitative measures for our empirical analysis (Sec. 3.3).

### 3.1 Peculiar Observations

Graph classification is a widely studied problem with many public datasets available. As graph-level outlier detection is rarely studied with no available dataset, repurposing the graph classification datasets by downsampling one class as outlier can easily provide outlier detection tasks based on real-world samples. In this section, for the first time, we report several unexpected behaviors on various datasets created in this manner.

**Setup.** We present our analysis on 4 widely used binary graph classification datasets: DD, PROTEINS, NCI1, and IMDB, which can be obtained from the TUDataset repository<sup>2</sup> [21]. DD and PROTEINS are bioinformatics datasets, NCI1 is a molecular dataset and IMDB is a social network. Dataset statistics are summarized in Table 2, which can also be found at <https://chrsmrrs.github.io/datasets/docs/datasets/>. The performance flip and related issues are observed for the first 3 datasets, DD, PROTEINS, and NCI1, but not for IMDB, which is presented for comparison purposes.

We create two main variants of each dataset, by down-sampling one class or the other (denoted class 0 or class 1), at varying rates. For each variant, we repeat the down-sampling 10 times with different random seeds such that the results are not an artifact of a specific data split. Finally, we feed the kernel based graph embeddings to LOF, where the two-stage methods are denoted as WL+LOF and PK+LOF, and the GIN model is trained end-to-end based on OCSVM objective, denoted OCGIN. We report results using  $L = 5$  for all models unless otherwise noted.

**3.1.1 Peculiar Observation 1: Performance Flip.** The main observation we make in this work is that **the detection performances of the outlier models appear to depend significantly on which class is down-sampled**. Table 1 shows the ROC-AUC performance on all datasets, i.e. their two variants, at down-sampling rate 0.1 for all three methods.

**OBSERVATION 1 (PERFORMANCE GAP).** *A large ROC-AUC gap is observed between the two different down-sampled variants of DD, PROTEINS, and NCI1, consistently across all models.*

Strikingly, not only the methods perform well on one variant and poorly on the other, but their performance is simply worse than random (!) in the latter case – since random ordering would achieve an ROC AUC of 0.5 in expectation. Perhaps more intriguingly:

**OBSERVATION 2 (AUCs SUM APPROXIMATELY TO 1).** *The sum of the two ROC-AUC values on the two variants of each dataset is approximately equal to 1, consistently across all models.*

To understand this better, recall the probabilistic interpretation of the ROC-AUC: it is the probability of correctly ranking a random positive instance (i.e. outlier) above a random negative instance (i.e. inlier). Then these two observations together, which we refer to as the “performance flip” issue, suggest a *revised* statement: **the models always consider the graphs from one fixed class to be more outlier than those from the other, irrespective of which one is down-sampled**. In other words, it is not that the down-sampled class has impact on the performance, in contrast, the ranking by the models is agnostic to this so-called “ground-truth” but rather has

<sup>2</sup><https://chrsmrrs.github.io/datasets/>

Table 1. Average ROC-AUC performance (and standard deviation) of 3 different graph embedding based methods for graph outlier detection using 4 binary graph classification datasets. Each dataset has 2 down-sampled variants, where outliers are created by down-sampling one of two classes (class 0 or class 1) with rate= 0.1, averaged over 10 different down-samplings. **Performance flip observed** on DD, PROTEINS, and NCI1 for all outlier models, **where ROC-AUC is significantly larger on one variant than the other**. ROC-AUC values less than 0.5 are shown in **bold** as they indicate worse-than-random performance.

Dataset	Outlier Class	OCGIN	PK+LOF	WL+LOF
DD	0	0.712 (0.041)	0.801 (0.026)	0.815 (0.020)
	1	<b>0.350 (0.043)</b>	<b>0.240 (0.035)</b>	<b>0.186 (0.024)</b>
PROTEINS	0	0.685 (0.059)	0.564 (0.043)	0.664 (0.024)
	1	<b>0.362 (0.040)</b>	<b>0.447 (0.071)</b>	<b>0.276 (0.021)</b>
NCI1	0	<b>0.465 (0.033)</b>	<b>0.403 (0.030)</b>	<b>0.349 (0.022)</b>
	1	0.656 (0.031)	0.662 (0.023)	0.730 (0.012)
IMDB	0	0.515 (0.033)	0.543 (0.042)	0.651 (0.022)
	1	0.651 (0.032)	0.610 (0.053)	0.603 (0.038)

a pre-determined bias toward one (fixed) class. Notice that this happens to be class 1 on DD and PROTEINS and class 0 on NCI1.

We conclude with three remarks. First, note that although the ranking of models by performance differs from dataset to dataset, the performance-flip and AUCs-sum-approximately-to-1 behaviors are consistent across models. Second, the issue does not appear to be universal as it does not arise on IMDB (cf. Table 1), where all models are better than random on both variants. We provide comparative analysis on all datasets in Sec. 4. Lastly, as we expand our DeepGLAD library, we continue to observe the same issue for additional outlier models such as graph2vec [24] paired with LOF as well as other deep GNN based models, to be reported in future version of our article.

**3.1.2 Peculiar Observation 2: Invariance to Down-sampling Rate.** When down-sampling one class as outlier with a certain down-sampling rate, we would conjecture that a lower rate would make the outlier detection task easier as the density of outliers becomes lower. Fig. 3 shows the detection ROC-AUC of WL+LOF (with  $L = 5$  iterations) for various down-sampling rates, from 0.05 to 0.85, on both variants of all datasets. The conjecture appears to hold only for IMDB – on which performance flip is not observed. In contrast, the performance is strikingly flat on DD, PROTEINS, and NCI1. Similar results hold for PK+LOF and OCGIN on these three datasets (See Sec. 4).

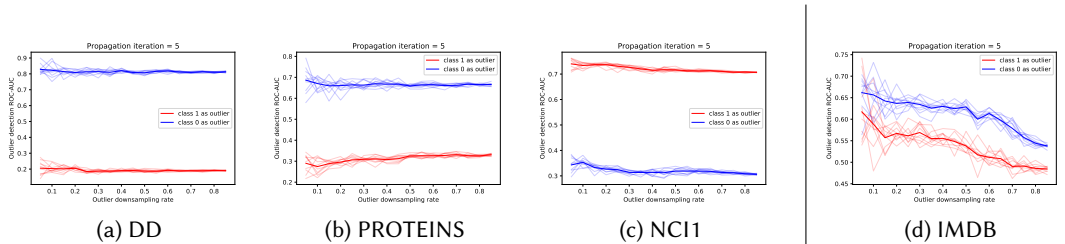


Fig. 3. Performance is invariant to downsampling rate on DD, PROTEINS, and NCI1 for WL+LOF. Similar behavior is observed for the other two methods.

**OBSERVATION 3 (INVARIANCE TO DOWN-SAMPLING RATE).** *Performance flip issue is not an artifact of the down-sampling rate, in fact, ROC-AUC appears to be invariant to the rate.*

This observation is in agreement with Observation 2 (AUCs-sum-approximately-to-1). The probabilistic interpretation is regarding *any two* random positive-negative instances, irrespective of the total number of instances from those groups.

**3.1.3 Peculiar Observation 3: Growing Performance Gap with Propagation.** Observation 3 is mainly related to a property of the dataset generation. On the other hand, a key property of the outlier models we employ in this work is the number of iterations (for WL and PK) or the number of layers (for GIN), earlier denoted with  $L$  (See Sec. 2.2), both of which correspond to propagations over the graph. Here we look at how the performance behaves under varying  $L$ . Fig. 4 shows the performance of WL+LOF on all datasets for two variants for  $L$  increased from 1 through 11. Results are qualitatively similar for PK+LOF, however OCGIN behaves differently (See Sec. 4).

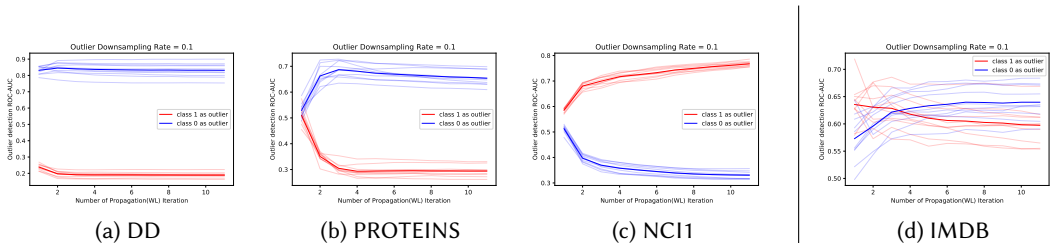


Fig. 4. **Performance gap between two variants tends to grow with increasing number of propagations** (i.e. iterations) of WL (subsequently paired with LOF), significantly on DD, PROTEINS, and NCI1. Similar behavior is observed for the PK-based model.

**OBSERVATION 4 (GROWING GAP WITH PROPAGATION).** *The difference in ROC-AUC performances on two different down-sampled variants of a classification dataset tends to grow with increasing number of graph propagations for WL- and PK-based outlier models. For OCGIN there exists no obvious growth.*

The growth is significant particularly on DD, PROTEINS, and NCI1 for which the performance flip occurs. It is interesting that this behavior is mainly associated with two-stage models and not with our end-to-end model. We can reason about the two-stage models based on the sparsification property that both exhibit. (In contrast, OCGIN is optimized where it is harder to reason about how the learning of its many parameters affects performance.) Recall that sparsification, as discussed in Sec. 2.2.1, implies that the kernel distance between two graphs tends to increase with the number of WL and PK iterations. In general, sparsity is expected to make the outlier detection task easier. It is, however, peculiar that sparsification appears to improve detection on only one of the down-sampled variants of DD, PROTEINS, and NCI1 (and seemingly also for IMDB, although not conclusively as the variances are quite large).

## 3.2 Hypothesis on Driving Mechanisms

Next we aim to build an understanding of the leading factors behind the unusual observations we have presented. To that end, we focus on investigating pairwise similarities – either produced by the graph kernel or the dot product between graph embeddings – normalized in range  $[0, 1]$ . We consider all-pairs similarities among all graphs before down-sampling. These convey important information about the density of and the distance between the graphs across classes, which many downstream outlier detectors rely on, including the two – LOF and OCSVM – we have used.

Fig. 5 shows the pairwise similarities among all graphs as well as how those change with increasing number of graph propagations (i.e. iterations) based on the WL subtree kernel. (Similar plots for PK and OCGIN can be found in Appendix Sec. A.) The pairwise similarities are block-wise grouped based on the true class label. We route attention to two factors:

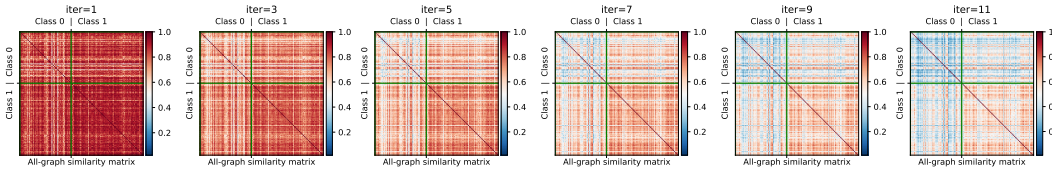


Fig. 5. Pairwise similarities among all graphs in DD dataset (graphs grouped by class) based on WL subtree kernel over increasing iterations (left to right).

1. *Diagonal, block-wise (intra-class) similarities:* Clearly sparsification arises for *both* classes, where the graphs within the same class become more and more dissimilar to one another as the number of iterations increases. What is even more important to note is that *the speed at which sparsification occurs is different for the two classes*. As shown in Fig. 5 for DD, distribution of graphs in class 0 sparsifies much faster than that for class 1, leading to a *disparity between class-level densities*. Although less apparent from the first subfigure, density disparity exists even after a single iteration. Increasing number of iterations only amplifies this disparity.
2. *Off-diagonal (inter-class) similarities:* Pairwise similarities among graphs within the sparser class (in Fig. 5, class 0 for DD) are *lower* than inter-class similarities on average. Put differently, graphs within the sparser class tend to look more similar to graphs in the other class than among themselves. This suggests that the class-level distributions of graphs in the embedding space have *overlapping support*.

Based on the above, we conjecture the following conditions as the leading factors behind our peculiar “performance flip” and related observations:

- (1) **(Growing) Density Disparity.** Density of outliers in the feature space is often inversely correlated with the difficulty of identifying them. That is, the more spread out and apart from inliers are the outliers, the easier the detection task gets. This suggests that designating as outliers the graphs from the sparser class (or the class that sparsifies faster) would induce a relatively easier task, as compared to graphs from the other class with higher density. What is more, graph propagation would contribute to a growing disparity between task difficulties, as density disparity grows with more propagation.
- (2) **Overlapping Support.** Density disparity alone is not a sufficient condition to explain the performance disparity (or flip) issue. Two sets of graph embeddings that are fully separable in the feature space would both induce an ‘easy’ task, no matter how different their within-set (i.e. class) densities are. Unsupervised graph representation learning methods, however, do not necessarily have the ability (at least explicitly) to embed graphs from the same class closely while maintaining inter-class separability. On the contrary, they tend to generate mixed embeddings that have a common/overlapping support among classes.

We conclude by forming the following hypothesis on the driving mechanisms behind “performance flip” and related observations. Provided graph embedding methods employed for outlier detection induce both density disparity as well as overlapping support, one down-sampling scenario creates a dense inlier distribution surrounded with dispersed outliers (‘easy’ task), whereas the other creates a sparse inlier distribution that has overlapping support with a small set of outliers with relatively higher density (‘hard’ task). Since most models assume the former scenario in their formalism, they ‘do well’ on the respective ‘easy’ task, and poorly on the other (Observation 1). More broadly, therefore, the performance flip issue stems from the (mis)alignment of data (i.e. inlier/outlier) distributions with the underlying assumptions of the detection models.

In fact, perhaps more disturbingly, the models tend to always consider the graphs from the sparser class to be more outlying than the graphs from the other, denser class – no matter *which* one is down-sampled and at what rate (Observation 3). That is, their probability of ranking a sparser-class instance above a denser-class instance remains almost the same, which leads to the observed AUCs-sum-approximately-to-1 behavior (Observation 2) and consequently, the worse-than-random performance when the denser class is down-sampled. The issue is exacerbated with more graph propagation as it leads to a growing disparity of densities and respective task difficulties (Observation 4).

### 3.3 Measures for Analysis

In the previous section we pointed out overlapping support and (growing) density disparity to be two key factors leading to the observed unusual behaviors. Here we introduce concrete measures to quantify these two factors.

- (1) **Qualitative visualization of overlapping support and growing density disparity:** Pairwise similarities do not directly reflect how points (i.e. graphs) are distributed in the representation space. We use multi-dimensional scaling (MDS) to map the graph embeddings into 2-dimensions (MDS mapping aims to preserve the relative pairwise similarities) wherein points from different classes are colored differently. Overlapping support can be validated visually from the mixing of two colors. On the other hand, the growing density disparity can be supported by the varying spread of points across classes and the rate at which this spread changes for each class across MDS visualizations corresponding to increasing propagation by a detector.

We remark that the MDS visualizations provide only qualitative evidence, as the mixing of colors and the varying spread of points could also be attributed to MDS error, i.e. could simply be artifacts; due to the space in which the pairwise similarities are to be preserved is constrained to only 2 dimensions for visualization purposes. Therefore, we also analyze quantitative measures of these factors described as follows.

- (2) **Quantitative measure of density disparity:** The distance between any two graphs from the sparse class would be larger. Therefore, we use the so-called *NN-Radius* to quantify the degree of density, defined as follows.

**Definition 3.1.** *NN-Radius is the distance (1-similarity as normalized in range  $[0, 1]$ ) to the  $k$ -th<sup>3</sup> nearest neighbor (NN) of a graph in the embedding space.*

A larger radius corresponds to lower local density. The distribution of the NN-radii of the graphs from each class measures the density of the class. A more left-shifted distribution would imply a denser class.

- (3) **Quantitative measure of overlapping support:** In the absence of overlap, assuming graphs from different classes are linearly well-separated in the embedding space (forming two disjoint clusters), we would expect the nearest neighbors of each graph to be from the same class. Therefore, we use the so-called *NN-Disagreement%* as the degree of overlap, defined as follows.

**Definition 3.2.** *NN-Disagreement% is the percentage of graphs from the opposite class within the NN-Radius of a graph.*

<sup>3</sup>In the paper we report results for  $k = 20$  and note that the take-aways are not sensitive to this choice.

We then study the distribution of NN-impurities of the graphs from each class. A left- or right-shifted distribution would respectively show whether a class is more likely to be surrounded by its own members (i.e. well-clustered, dense) or not (i.e. dispersed, sparse).

### 3.4 Simulations on $k$ -regular Graphs

In this section we perform various simulations to better understand the disparity in sparsification rates between two classes, that is how one sparsifies faster than the other (See e.g. Fig. 5). We use WL subtree kernel for the simulations as these do not require any parameter training and hence are easier to analyze. The simulations are designed to show: (1) Even a small difference between two graphs can be amplified by propagation, leading to sparsification; and (2) Various factors, including differences in label distribution and topology, contributes to differences in the rate of sparsification between two classes.

We consider simulations on  $k$ -regular graphs where each node has exactly  $k$  number of neighbors, i.e. the same degree. (Unlabeled)  $k$ -regular graphs are among the class of graphs on which 1-dimensional WL (1-WL) isomorphism test [34] fails to reject non-isomorphism. That is, 1-WL test cannot distinguish two structurally non-isomorphic  $k$ -regular graphs. In practice, node/edge labels or attributes may help diminish such difficulty by breaking the symmetry [15]. This is exactly the route we take to induce asymmetry in a controlled fashion (from low to high). Specifically, we design two cases:

- **Case 1:** We start with two identical  $(k, n)$  regular graphs ( $n$  nodes, all with degree= $k$ ), where all nodes are labeled  $A$ . Then, we flip the labels of  $m$  randomly chosen nodes in each graph to  $B$ . As such, the graphs are structurally isomorphic, whereas  $B$ -labeled nodes are ensured to induce asymmetry (and hence non-isomorphism) between the graphs.
- **Case 2:** We start with two identical  $(k, n)$  regular graphs, where the nodes are labeled with two different labels,  $A$  or  $B$ . To induce non-isomorphism, we perform degree-preserving rewiring between  $r$  randomly chosen edge pairs in one of the graphs.

Our goal is to start from a place where WL distance is zero (i.e. identical graphs) and to study the effect of increasing  $m$  or  $r$  on the distance growth. Fig. 6(a) illustrates Case 1 on two so-called Petersen graphs ( $k = 3, n = 10$ ) where  $m = 1$  node’s label in each graph is flipped from gray (label  $A$ ) to red (label  $B$ ), inducing non-isomorphism. Case 2 is illustrated in (b) where we rewire  $r = 1$  edge pair in one graph (right) to create a graph that is non-isomorphic to the other (left) graph.

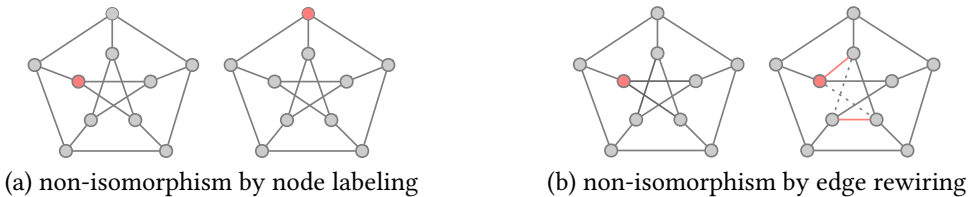


Fig. 6. Non-isomorphism is induced (a) between two unlabeled Petersen graphs by flipping node labels asymmetrically, and (b) between two labeled Petersen graphs by degree-preserving edge rewiring.

Without the perturbations (label flipping in Case 1, and rewiring in Case 2), WL distance between the two graphs would be equal to zero in both cases, irrespective of number of iterations. Just a small change, as shown in Fig. 6, “jump-starts” WL where the distance between the graphs starts growing with increasing WL iterations.

In Fig. 7 (a) and (b) we show how graph distance changes with increasing WL iterations as a function of number of node labels flipped in Case 1 and number of edge pairs rewired in Case 2, respectively. Notice that even after a relatively small perturbation on otherwise non-distinguishable graphs, their distance grows over iterations. The bigger the amount of perturbation (i.e. the difference between two graphs), the larger the distances as reflected by WL, and also the larger the growth rate (reflected with the increasing gap between curves).

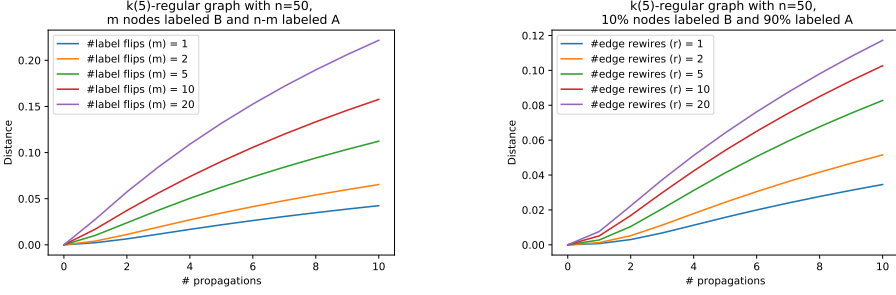


Fig. 7. Distance between two  $k$ -regular graphs ( $k = 5$ ,  $n = 50$ ) as a function of (left, Case 1) number of node labels flipped, and (right, Case 2) number of edge pairs rewired. Each curve is averaged over 100 rounds to remove randomness.

The distance growth is also a consequence of graph topology. Fig. 8(a) shows graph distance over WL iterations on  $k$ -regular graphs with varying  $k$ , when number of label flips is fixed to  $m = 5$  in Case 1. Similarly, Fig. 8(b) shows the same when the number of edge rewirings is fixed to  $r = 10$  in Case 2. In both cases the graph distances are larger for increasing  $k$  across iterations. These show that the effect on distance of the same (even a small) amount of perturbation on two graphs varies depending on the topology.

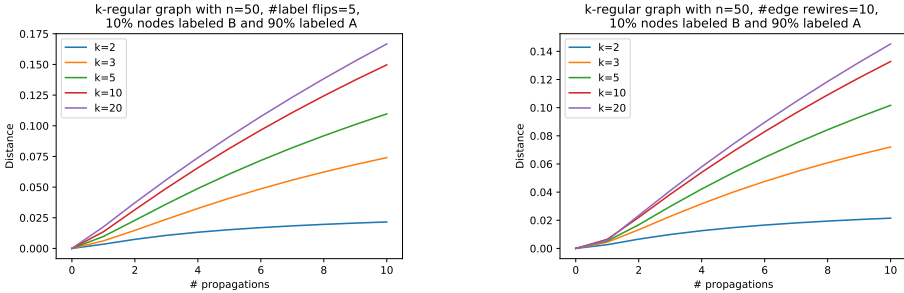


Fig. 8. Distance between two  $k$ -regular graphs ( $n = 50$ ) as a function of  $k$  for (left, Case 1) when  $m = 5$  node labels are flipped, and for (right, Case 2) when  $r = 10$  edge pairs are rewired. Each curve is averaged over 100 rounds to remove randomness.

All in all, sparsification is evident from our simulations – i.e. distances grow over iterations, or graph propagations. The growth rate of sparsification is sensitive to various factors (difference in label distribution, difference in topology, etc.). It is unlikely that real-world classes would consist of graphs with exactly the same variation for all factors. Therefore, it is not a freak occurrence that on average the distance between two graphs in one class sparsifies at a different rate than between those in another class. In fact, it is the opposite – it would be quite a coincidence for graphs from two different classes to sparsify at exactly the same rate. As a result, class-level density disparity as discussed in Sec. 3.2 appears to be an inevitable consequence of using these types of representation learning techniques.

## 4 EMPIRICAL ANALYSIS

To reiterate, we hypothesize that the performance flip issue occurs when samples from different classes have large enough density disparity and overlapping support. Provided those two conditions hold, outlier models tend to rank the sparser class above the denser class no matter which class is down-sampled at what rate. In this section, we present further measurement and quantitative analysis to support our hypothesis. We first introduce the setup in detail regarding model configurations and then present empirical results for two cases: for datasets with performance flip (DD, PROTEINS, and NCI1) and the other without (IMDB).

### 4.1 Experiment Setup

Table 2. Dataset summary statistics.

Dataset	GraphType	Class	#Graphs	#NodeLabels	Avg. #Nodes	Avg. #Edges	Avg. Degree
DD	Labeled	0	691	89	355.2	1806.6	5.04
		1	487	89	183.7	898.8	4.88
PROTEINS	Labeled	0	663	3	50	188.1	3.79
		1	450	3	22.9	83.1	3.64
NCI1	Labeled	0	2053	37	25.65	55.3	2.15
		1	2057	37	34.07	73.9	2.17
IMDB	Degree-Labeled	0	500	136	20.1	193.5	9.1
		1	500	136	19.4	192.5	8.6

**Datasets.** As mentioned in Sec. 3.1 we perform empirical analysis based on 4 binary graph classification datasets, namely DD, PROTEINS, NCI1, and IMDB-BINARY from TUDataset repository [21]. Table 2 gives summary statistics. Our analysis use both full data and 2 down-sampled variants of each dataset with down-sampling rate=0.1.

**Model configuration.** Our experiments are based on two-stage models WL+LOF and PK+LOF, as well as end-to-end deep-one-class model OCGIN. We study the behavior of these models under different number of propagations; specifically WL and PK iterations range from 1 to 11, and OCGIN embeddings are extracted from layers 0 (i.e. input node vectors) through 5. PK has a bin-width hyperparameter for hash function  $\phi_{PK}$  (See Eq. 3), which is set to 0.1. Note that smaller bin-width leads to faster sparsification with a more severe performance flip. The LOF outlier detector is setup with default parameters ( $k=20$  number of neighbors, leaf size 30) from scikit-learn [28]. For OCGIN we use the default GIN implementation from [35], where we remove bias terms at all layers to prevent feature collapse [30]. A graph’s representation is produced from the summation of all previous layers’ hidden representations, with a mean pooling over all nodes in the graph. Note that we train OCGIN only on down-sampled variants of a dataset, as it is trained end-to-end assuming outliers to be minority. For figures utilizing full data, we simply feed-forward all the graphs in the database over the *trained* model. We set number of layers to  $L=5$  and number of hidden units to 128 for all datasets. We use the Adam optimizer [13] to train OCGIN with a  $5 \cdot 10^{-4}$   $L_2$  penalty on weights. The model is trained for 25 epochs. All other hyperparameters are picked from typical/default values, since our goal is to illustrate the performance flip and related issues instead of achieving best performance. Hyperparameter selection for unsupervised deep outlier detection is an important problem which is outside the scope of this paper.

**Pairwise similarity matrix.** Our proposed measures in Sec. 3.3 are computed on top of pairwise similarities among all graphs. For PK and WL kernels, the normalized kernel matrix is investigated. For OCGIN, where we only have access to graph embeddings, we calculate pairwise similarity as  $(1 - \text{normalized pairwise distance})$  between two graphs, using Euclidean distance (i.e.  $L_2$  norm). Similarity matrix is normalized to range  $[0, 1]$  via dividing it by the largest element in the matrix.

**Remark.** We include all figures corresponding to those presented in the following as well as previous sections for all 3 models on all 4 datasets in the Appendix. Only a subset of them are presented in the main paper for brevity.

## 4.2 Analysis of Datasets with Performance Flip

**4.2.1 Analysis on full data.** We start with analyzing the inherent differences between two classes regarding density on DD. Fig. 9 (top row) visualizes the all-pairs similarity matrix based on WL over increasing iterations where sparsification can be observed for both classes (left to right). In the second row, 2-d MDS embeddings of all the graphs based on the corresponding pairwise similarities are shown. Again sparsification can be visually confirmed based on the increasing spread of points (i.e. graphs) in each class. In addition, we notice that class 0 (green points) *sparsify faster* than class 1 (orange points), as the denser class 1 instances are surrounded by the dispersed class 0 instances. We quantify this difference via the *NN-Radius* measure, as in the third row, where the corresponding distributions of *NN-Radius* for all graphs are shown for each class. Over iterations both class distributions shift to the right (i.e. sparsify). The shift is more evident for class 0 (i.e.

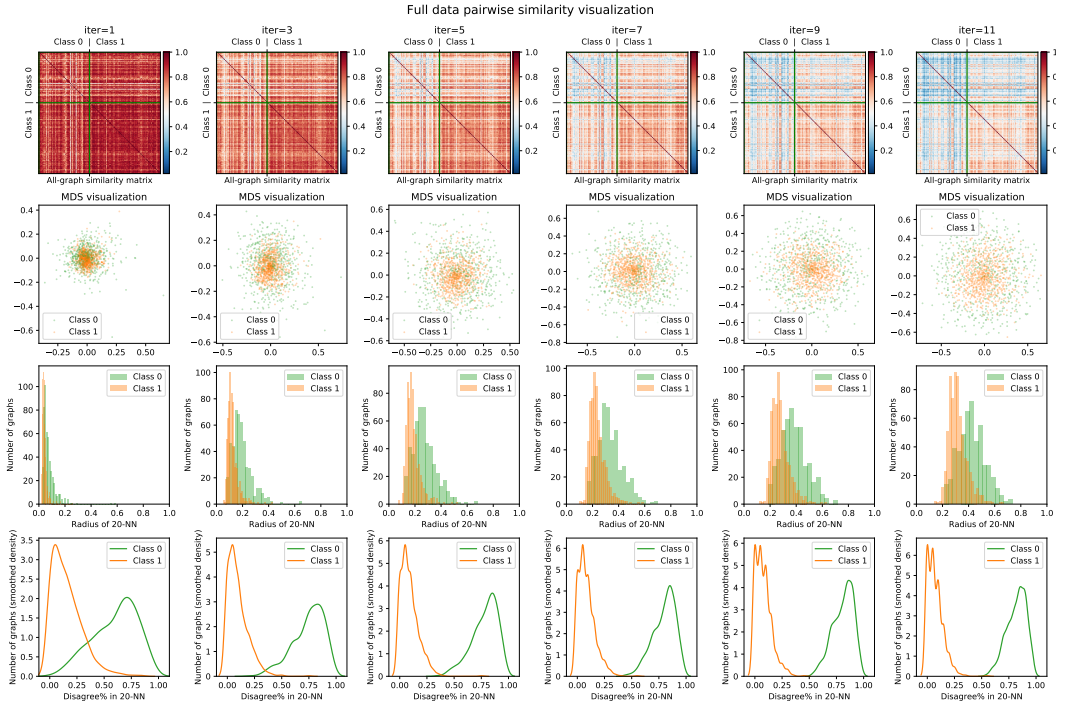


Fig. 9. (Top row) Pairwise similarity matrix for all graphs in full DD dataset, based on WL subtree kernel over increasing iterations (left to right). (Second row) 2-d MDS visualization based on the similarity matrix. (Third row) Distribution of *NN-Radius* for all graphs in each class. (Last row) Distribution of *NN-Disagreement%* for all graphs in each class.

speed of sparsification is larger) as the (green) histogram spreads out while the other (orange) histogram remains relatively peaked.

Next we analyze the overlapping support between two classes. The mixing of colors in the MDS visualizations is suggestive of overlap, however one can argue that it is an artifact of limited representation capacity of MDS in 2-d. To quantify overlap more concretely, we show the distributions of *NN-Disagreement%* for all graphs in each class in the last row of Fig. 9. The distributions for class 1 concentrate more on the left side (majority of neighbors are from the *same* class) whereas for class 0 they concentrate on the right (majority of neighbors are from the *opposite* class). Both density disparity and overlapping support are increasingly more evident with increasing number of iterations, which suggests that graph propagation amplifies the issue.

To summarize, this analysis confirms that class 0 in DD is the increasingly sparser class with larger *NN-Radius* (means sample density is smaller) and higher *NN-Disagreement%* (means higher overlapping support). As a result, down-sampling class 0 as outlier induces a relatively ‘easy’ task for WL+LOF. Moreover, the task becomes ‘easier’ with more propagation as the graphs in class 0 spread out even further, hence the increasing performance gap.

The conclusions are similar for PK on DD, as shown in Fig. 10(a). For OCGIN, while we continue to observe performance flip on DD variants, it is to a lesser degree. Specifically we find that the disparity between classes is not worsened with increasing graph propagation in this case, as suggested by Fig. 10(b). In fact, the difference in distributions seems to close especially at the last layer. Irrespectively, OCGIN performs considerably better when class 0 is down-sampled like the

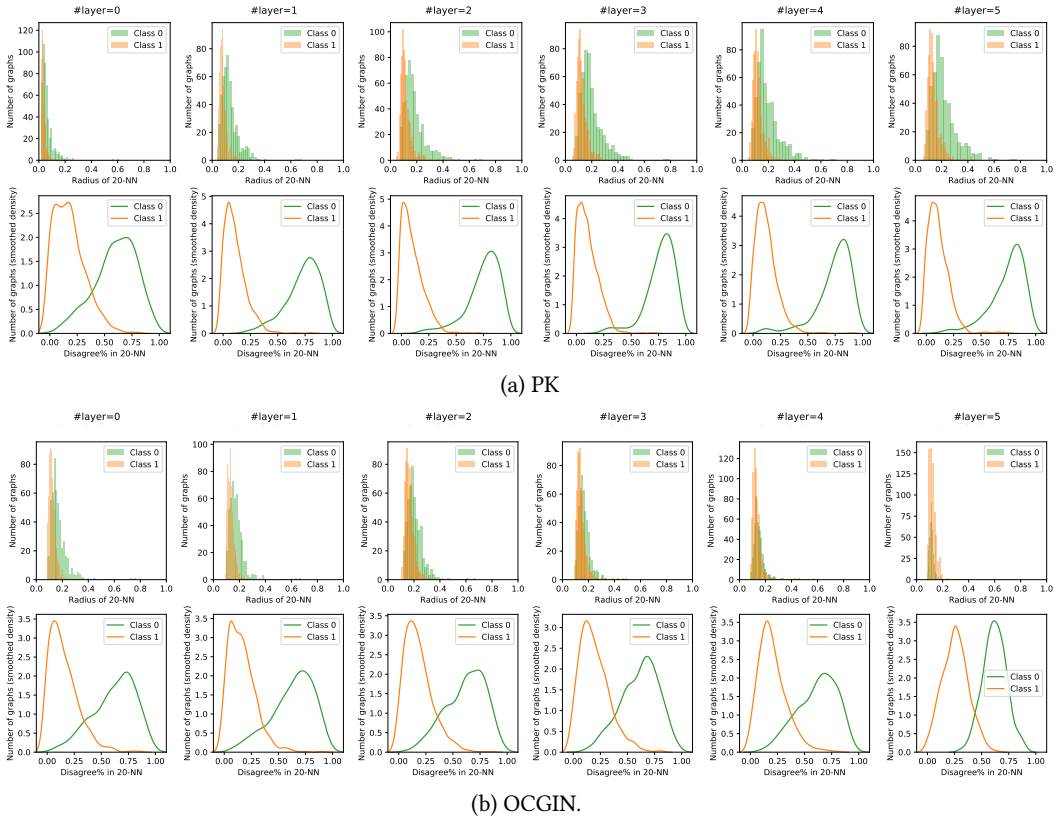


Fig. 10. Quantitative measures of density disparity and overlapping support on DD for (a) PK and (b) OCGIN for increasing graph propagation (left to right).

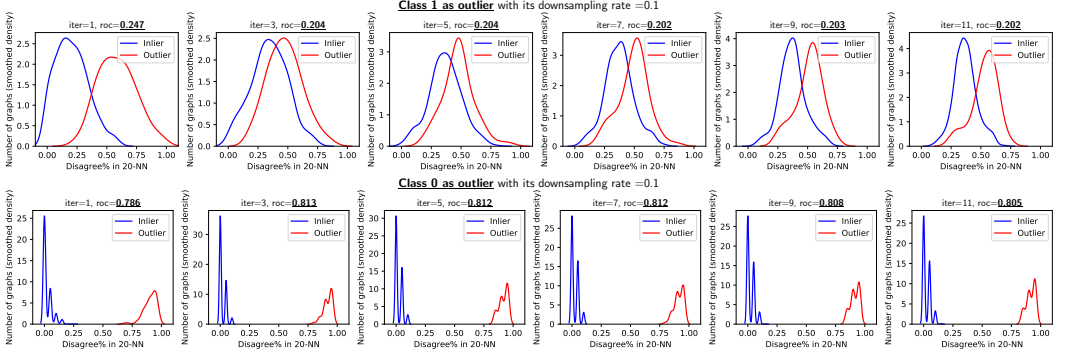


Fig. 11. *NN-Disagreement%* distribution of outliers (top row: class 1 is down-sampled and bottom row: class 0 is down-sampled, in red) and inliers (vice versa, in blue) over WL iterations (left to right) on DD.

other models, meaning that it is not shielded from the performance flip issue that we identify. We believe this is due to the initial disparity (See Fig. 10(b) at layer 0, i.e. original input), which it cannot recover from, despite model training. This is akin to a bad initialization (for one variant) of OCGIN that ultimately leads to poor performance.

**4.2.2 Analysis upon down-sampling.** Next we analyze the flip in performance upon down-sampling one class or the other via the contrast in *NN-Disagreement%* distributions. Fig. 11(top) and (bottom) respectively show those distributions when class 1 is down-sampled (denoted Outlier in red) and when class 0 is down-sampled (now denoted Outlier in red) for WL on DD. We notice the stark difference: At the (bottom), the inliers form a dense distribution with negligible mixing with the outliers. The outliers are dispersed, far from one another, as their *NN-neighborhood* mainly contains inliers. This is the ‘easy’ detection task that well aligns with the underlying assumption of most outlier detectors – hence the high performance of WL+LOF.

In contrast, the (top) figures suggest that the inliers and outliers are intermixed, which worsens with propagation as the distributions become more and more indistinguishable. (Note that down-sampled class inherently has a right-shifted distribution as down-sampling induces sparsity.) This corresponds to the ‘hard’ detection task where it is difficult to distinguish inliers from outliers – hence the poor, in fact worse-than-random performance.

The conclusions are similar for WL+LOF on PROTEINS and NCI1, as shown in Fig. 12(a) and (b), respectively (except for NCI1 down-sampling class 0 happens to induce the ‘hard’ task). In fact, performance appears to be inversely correlated with the amount of overlap between the *NN-Disagreement%* distributions of inliers and outliers. We refer to the Appendix for similar results on these three datasets for PK+LOF and OCGIN.

### 4.3 Analysis of Dataset without Performance Flip

Although the performance flip issue occurred on a considerable number of datasets we have experimented with, it is not always observed. In this section, we present a similar analysis for IMDB-BINARY for comparison purposes.

As shown in Fig. 13, sparsification arises rather fast on IMDB-BINARY with increasing WL iterations – notice the drastic shift of the *NN-Radius* distributions from left-most to right-most (third row). This can also be visually confirmed from the pairwise similarity matrix (top row) as the heatmap gets darker blue (from left to right). Interestingly, the rate (or speed) of sparsification appears to be similar among the two classes. As such, density disparity does not seem to arise –

## On Using Classification Datasets to Evaluate Graph Outlier Detection: Peculiar Observations and New Insights

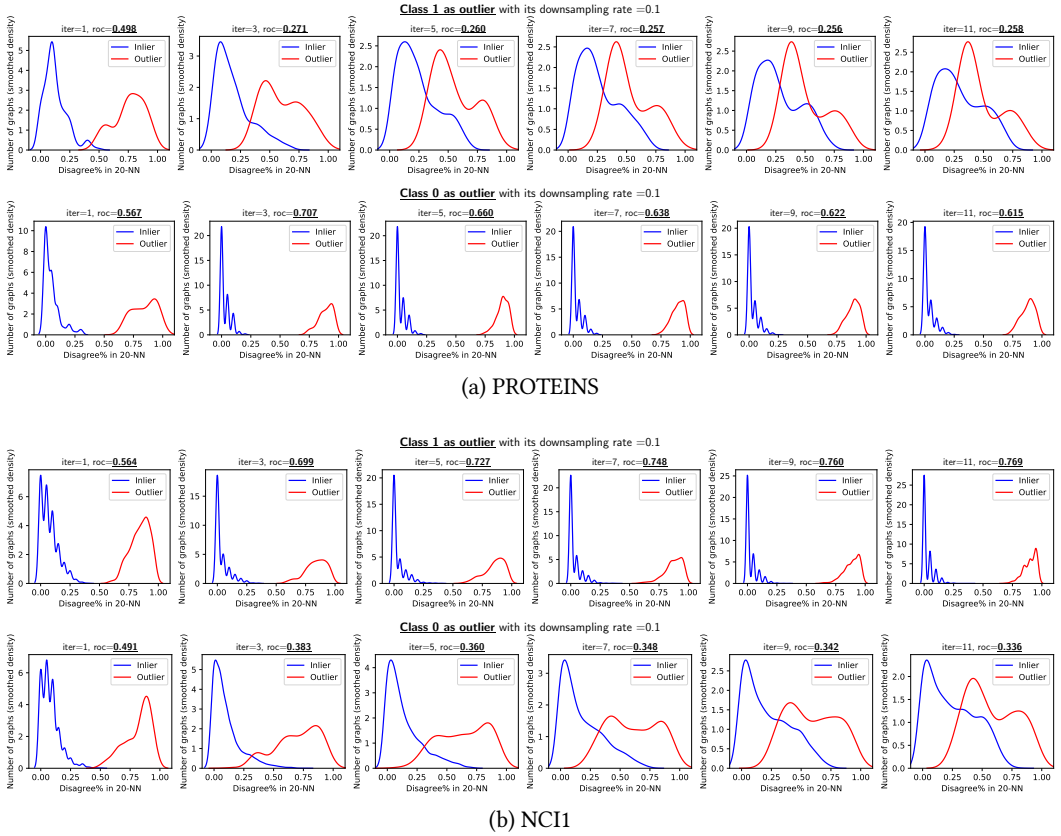


Fig. 12. *NN-Disagreement%* distribution of outliers (top rows: when class 1 is down-sampled and bottom rows: when class 0 is down-sampled, in red) and inliers (vice versa, in blue) over WL iterations (left to right) on (a) PROTEINS and (b) NCI1.

notice the similar mixing among the colored points in 2-d MDS visualization (second row). On the other hand, we continue to observe the overlapping support (i.e. mixing) of graph embeddings to a large extent (last row).

These suggest that down-sampling any one of the classes as outlier would induce two detection tasks with similar difficulty. Fig. 14 confirms this hypothesis, where the distribution of inliers and outliers in the embedding space look similar between the two down-sampled variants of IMDB-BINARY. Moreover, the outliers are sparser and more dispersed as compared to the inliers, which consequently leads to better-than-random performance on both tasks. The ROC-AUC values are not too high due to the mixing of the embeddings that makes the detection task harder. In Sec. 3.2 we argued that density disparity alone is not a sufficient condition for performance flip. This result on IMDB-BINARY shows that overlapping support (i.e. mixing) alone is also not a sufficient condition for the performance flip. Both conditions together give rise to the issue.

To conclude, our analysis sheds light onto the leading factors (density disparity and overlapping support) as well as contributing factors (graph propagation) behind the performance flip issue. These help us reason about both cases in which it occurs or not. However, we do not have a full understanding of why these factors arise for some datasets but not the others in the first place. Future research could focus on studying this disparity between datasets.

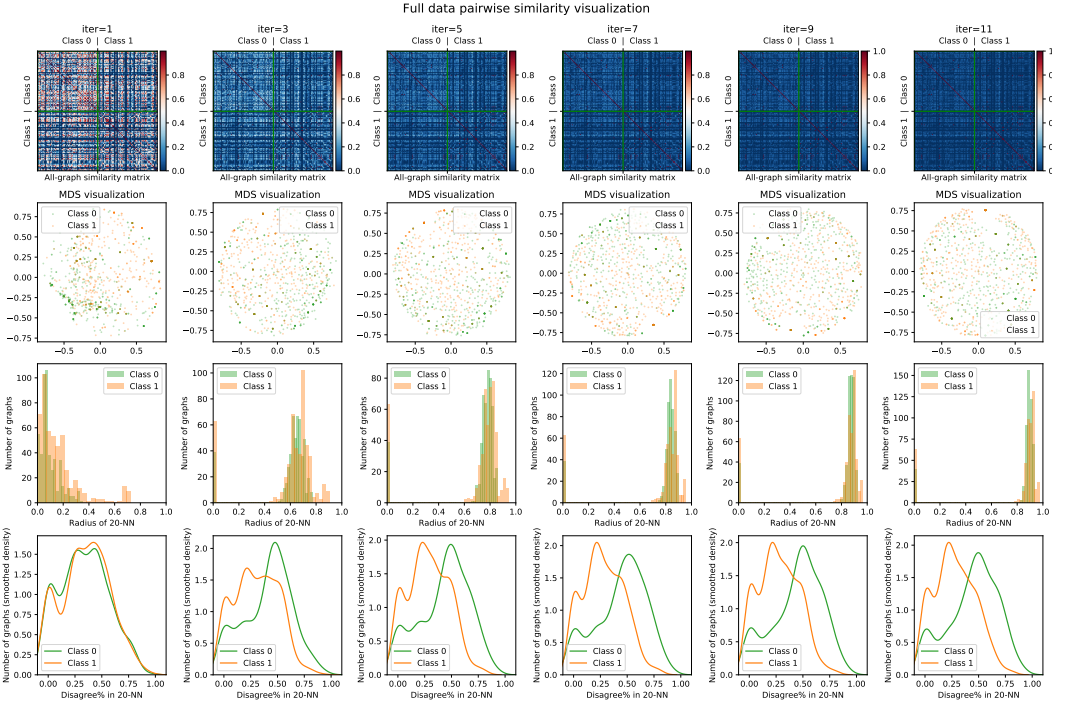


Fig. 13. (Top row) Pairwise similarity matrix for all graphs in full IMDB-BINARY dataset, based on WL subtree kernel over increasing iterations (left to right). (Second row) 2-d MDS visualization based on the similarity matrix. (Third row) Distribution of  $NN$ -Radius for all graphs in each class. (Last row) Distribution of  $NN$ -Disagreement% for all graphs in each class.

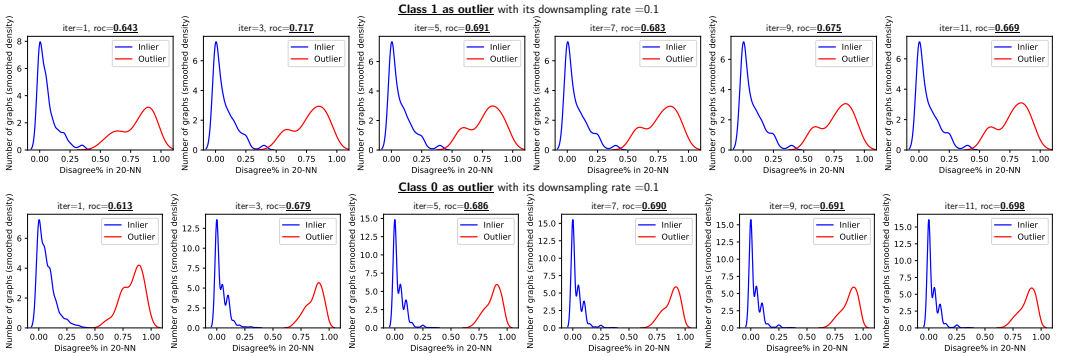


Fig. 14.  $NN$ -Disagreement% distribution of outliers (top row: class 1 is down-sampled and bottom row: class 0 is down-sampled, in red) and inliers (vice versa, in blue) over WL iterations (left to right) on IMDB-BINARY.

## 5 DISCUSSION OF THE FINDINGS

The findings in our paper are studied in the context of graph-level outlier detection, which stands at the intersection of graph representation learning and outlier detection. On one hand, performance flip driven by the misalignment between the graph representations produced by propagation/substructure based models and the underlying assumptions of outlier detectors becomes an

obstacle for effectively solving the graph-level outlier detection problem. On the other hand, it also raises a ‘red flag’ regarding potentially broader problems in these two widely studied fields: outlier detection and graph representation learning.

Repurposing classification datasets as outlier detection benchmarks is widely used in outlier detection considering its convenience and availability of labels, however there is limited understanding of the inherent properties of classification datasets and whether they would introduce any bias (other than those reported here) for evaluating outlier detectors. As for graph representation learning, while the field is booming with the advances in graph neural networks, the issues regarding class density disparity, sparsification, and mixing (or overlap) of embeddings in the representation space bring about other important deliberations.

To the best of our knowledge, our findings have not been reported in any prior work. Arguably, we believe that the issues we have identified have broader implications for graph classification and graph-level clustering using graph neural networks, and the potential to open new directions of future work in both fields. We discuss the potential implications of our findings respectively for outlier detection and graph representation learning as follows. More rigorous analysis is needed to confirm or confute these arguments.

### 5.1 Impact on Outlier Detection

Most traditional outlier detectors are designed for low-dimensional point-cloud (i.e. vector) datasets based on specific assumptions of the behavior in input space. With the emergence of large-scale high-dimensional and highly structured data such as images, text, time series, and so on (e.g. in medical records), deep anomaly detection has emerged as a promising area of research [4, 27, 29]. Irrespectively, most detection models assume outliers to ‘live’ in low-density regions of the space. In contrast, as our findings reveal, repurposing classification datasets for outlier model evaluation often creates a setting in which this assumption is violated. In fact the setting in which the so-called outlier samples form a higher density region than the inliers is studied under a different area called rare category discovery [12].

Moreover, our findings have a close connection with graph representations as generated by propagation based models. This motivates the design of better graph representation learning techniques for outlier detection, particularly those that do not exhibit similar pitfalls.

Our study focused on binary graph classification datasets, however the issues would arguably extend to multi-class scenarios where two or more classes are subsampled to construct the outliers. Although the possibility of all down-sampled classes to violate the sparsity assumption would be reduced, the model errors could still be biased (i.e. skewed) toward the ones that exhibit the issues we have reported. Finally, more research is called for the transferability of our findings to non-graph settings.

### 5.2 Impact on Tasks Relying on Graph Representation

In early days, propagation or substructure based graph information gathering methods have been designed originally for the graph isomorphism test. Recently, the effectiveness of the Weisfeiler-Leman test of isomorphism [34] motivated researchers to develop graph representation learning techniques using substructures, including many graph kernels<sup>4</sup> and graph neural networks. The exceptional discriminating ability of propagation based graph representation is a blessing. However, as we find in this work, it can also be a curse: the graphs from the same class can be widely spread out in the representation space instead of being well-clustered.

<sup>4</sup>Specifically R-convolution kernels that decompose the graphs into their “parts”, and compare all pairs of these “parts” using existing kernels [26].

The authors of the Graph Isomorphism Network (GIN) [35] have claimed GIN to be “the most expressive [architecture] among the class of GNNs” because it can be as discriminative as the WL graph isomorphism test. We challenge this viewpoint: the discriminating ability of the WL test may not be suitable to be built into graph representation learning when used for tasks that expect well-clustered data in the feature space. In particular, (graph-level) clustering would work well for well-clustered data with clear cluster boundaries – which would be adversely affected by the mixing (i.e. overlap) and sparsification issues we have identified. In addition, graph classification would work well provided distinguishable class manifolds that are densely sampled from (to be able to learn discriminative class boundaries) – for which mixing and sparsity would be deteriorating, where a small amount of sparsely sampled training data from a class would not be representative of the support region of the class and would lead to poor generalization. We believe the conflict in viewpoints arises as we draw attention to graph-level tasks whereas a vast body of prior work on representation learning, including GIN, focused on *node-level* tasks (i.e. node embedding). More research is called for the expressive power of various *graph* embedding techniques.

## 6 CONCLUSION

In this work we identified the (what we call) *performance flip* issue with repurposing binary graph classification datasets for evaluating outlier detection models, including graph kernel and graph neural network based models. While down-sampling one class to constitute the outliers yields relatively high ROC-AUC performance for the models, down-sampling the other yields significantly worse (in fact, worse than random) performance, irrespective of the down-sampling rate. The performances on these two variants approximately sum to 1, implying one of the classes is always deemed more outlying irrespective of *which* one is down-sampled.

It is easy to state that one variant induces a relatively easier task that aligns well with the underlying assumptions of the models, and the other variant does not. Through careful analysis, we find that the driving factors behind the issue are two: (1) disparity between class-level densities (or within-class sample similarity), and (2) overlapping support of the density distributions. We also find specifically for kernel based models that graph propagation, and the associated sparsification property, is a contributing factor that amplifies the disparity and ultimately the performance gap.

The performance flip issue does not arise on all datasets. Future research could focus on demystifying this disparity, this time between the datasets. The extent to which our findings apply to non-graph settings or to multi-class classification datasets also warrant future work.

Our findings have implications for the fair and effective evaluation of outlier models. Our analysis provides tools for better understanding the datasets used for benchmark evaluation. We also shed light onto the effect of graph propagation on the distribution of graph embeddings, which we argued to likely have further implications for graph classification and clustering tasks. To facilitate future research on these and related issues, we release a deep graph-level anomaly detection library and all datasets used in this work at <https://tinyurl.com/deeplad>.

## ACKNOWLEDGMENTS

This research is sponsored by NSF CAREER 1452425. We thank Charu Aggarwal for helpful discussions and critical reading of the manuscript. DeepGLAD Library was partly built during the first author’s internship at IBM T. J. Watson Research Center. Conclusions expressed in this material are those of the authors and do not necessarily reflect the views, expressed or implied, of the funding and other parties involved.

## REFERENCES

- [1] Charu C Aggarwal. 2015. Outlier analysis. In *Data mining*. Springer, 237–263.

- [2] Markus M Breunig, Hans-Peter Kriegel, Raymond T Ng, and Jörg Sander. 2000. LOF: identifying density-based local outliers. In *Proceedings of the 2000 ACM SIGMOD international conference on Management of data*. 93–104.
- [3] Guilherme O Campos, Arthur Zimek, Jörg Sander, Ricardo JGB Campello, Barbora Micenkova, Erich Schubert, Ira Assent, and Michael E Houle. 2016. On the evaluation of unsupervised outlier detection: measures, datasets, and an empirical study. *Data mining and knowledge discovery* 30, 4 (2016), 891–927.
- [4] Raghavendra Chalapathy and Sanjay Chawla. 2019. Deep Learning for Anomaly Detection: A Survey. <http://arxiv.org/abs/1901.03407> cite arxiv:1901.03407.
- [5] Kaize Ding, Jundong Li, Rohit Bhanushali, and Huan Liu. 2019. Deep anomaly detection on attributed networks. In *Proceedings of the 2019 SIAM International Conference on Data Mining*. SIAM, 594–602.
- [6] Andrew Emmott, Shubhomoy Das, Thomas Dietterich, Alan Fern, and Weng-Keen Wong. 2015. A meta-analysis of the anomaly detection problem. *arXiv preprint arXiv:1503.01158* (2015).
- [7] Andrew F Emmott, Shubhomoy Das, Thomas Dietterich, Alan Fern, and Weng-Keen Wong. 2013. Systematic construction of anomaly detection benchmarks from real data. In *Proceedings of the ACM SIGKDD workshop on outlier detection and description*. 16–21.
- [8] Ines Färber, Stephan Günemann, Hans-Peter Kriegel, Peer Kröger, Emmanuel Müller, Erich Schubert, Thomas Seidl, and Arthur Zimek. 2010. On using class-labels in evaluation of clusterings. In *MultiClust: 1st international workshop on discovering, summarizing and using multiple clusterings held in conjunction with KDD*. 1.
- [9] Aristides Gionis, Piotr Indyk, and Rajeev Motwani. 1999. Similarity Search in High Dimensions via Hashing. In *The VLDB Journal*. 518–529. <http://citeseer.ist.psu.edu/203242.html>
- [10] Christopher R Harshaw, Robert A Bridges, Michael D Iannacone, Joel W Reed, and John R Goodall. 2016. Graphprints: Towards a graph analytic method for network anomaly detection. In *Proceedings of the 11th Annual Cyber and Information Security Research Conference*. 1–4.
- [11] Douglas M Hawkins. 1980. *Identification of outliers*. Vol. 11. Springer.
- [12] Jingrui He. 2012. *Analysis of Rare Categories*. Springer. <https://doi.org/10.1007/978-3-642-22813-1>
- [13] Diederik P Kingma and Jimmy Ba. 2014. Adam: A method for stochastic optimization. *arXiv preprint arXiv:1412.6980* (2014).
- [14] Thomas N. Kipf and Max Welling. 2017. Semi-Supervised Classification with Graph Convolutional Networks. In *International Conference on Learning Representations (ICLR)*.
- [15] Pan Li, Yanbang Wang, Hongwei Wang, and Jure Leskovec. 2020. Distance Encoding: Design Provably More Powerful Neural Networks for Graph Representation Learning. *arXiv e-prints*, Article arXiv:2009.00142 (Aug. 2020), arXiv:2009.00142 pages. arXiv:2009.00142 [cs.LG]
- [16] Chao Liu, Xifeng Yan, Hwanjo Yu, Jiawei Han, and Philip S Yu. 2005. Mining behavior graphs for “backtrace” of noncrashing bugs. In *Proceedings of the 2005 SIAM International Conference on Data Mining*. SIAM, 286–297.
- [17] Fei Tony Liu, Kai Ming Ting, and Zhi-Hua Zhou. 2008. Isolation forest. In *2008 Eighth IEEE International Conference on Data Mining*. IEEE, 413–422.
- [18] Larry M Manevitz and Malik Yousef. 2001. One-class SVMs for document classification. *Journal of machine Learning research* 2, Dec (2001), 139–154.
- [19] Amir Markovitz, Gilad Sharir, Itamar Friedman, Lihi Zelnik-Manor, and Shai Avidan. 2020. Graph Embedded Pose Clustering for Anomaly Detection. In *Proceedings of the IEEE/CVF Conference on Computer Vision and Pattern Recognition*. 10539–10547.
- [20] Federico Monti, Fabrizio Frasca, Davide Eynard, Damon Mannon, and Michael M Bronstein. 2019. Fake news detection on social media using geometric deep learning. *arXiv preprint arXiv:1902.06673* (2019).
- [21] Christopher Morris, Nils M Kriege, Franka Bause, Kristian Kersting, Petra Mutzel, and Marion Neumann. 2020. TUDataset: A collection of benchmark datasets for learning with graphs. *arXiv preprint arXiv:2007.08663* (2020).
- [22] Annamalai Narayanan, Mahinthan Chandramohan, Lihui Chen, Yang Liu, and Santhoshkumar Saminathan. 2016. sub-graph2vec: Learning distributed representations of rooted sub-graphs from large graphs. *arXiv preprint arXiv:1606.08928* (2016).
- [23] Annamalai Narayanan, Mahinthan Chandramohan, Rajasekar Venkatesan, Lihui Chen, Yang Liu, and Shantanu Jaiswal. 2017. graph2vec: Learning distributed representations of graphs. *arXiv preprint arXiv:1707.05005* (2017).
- [24] Annamalai Narayanan, Mahinthan Chandramohan, Rajasekar Venkatesan, Lihui Chen, Yang Liu, and Shantanu Jaiswal. 2017. graph2vec: Learning Distributed Representations of Graphs. *CoRR* abs/1707.05005 (2017). <http://dblp.uni-trier.de/db/journals/corr/corr1707.html#NarayananCVCLJ17>
- [25] Marion Neumann, Roman Garnett, Christian Bauckhage, and Kristian Kersting. 2016. Propagation kernels: efficient graph kernels from propagated information. *Machine Learning* 102, 2 (2016), 209–245.
- [26] Giannis Nikolentzos, Giannis Siglidis, and Michalis Vazirgiannis. 2019. Graph Kernels: A Survey. *CoRR* abs/1904.12218 (2019). <http://dblp.uni-trier.de/db/journals/corr/corr1904.html#abs-1904-12218>

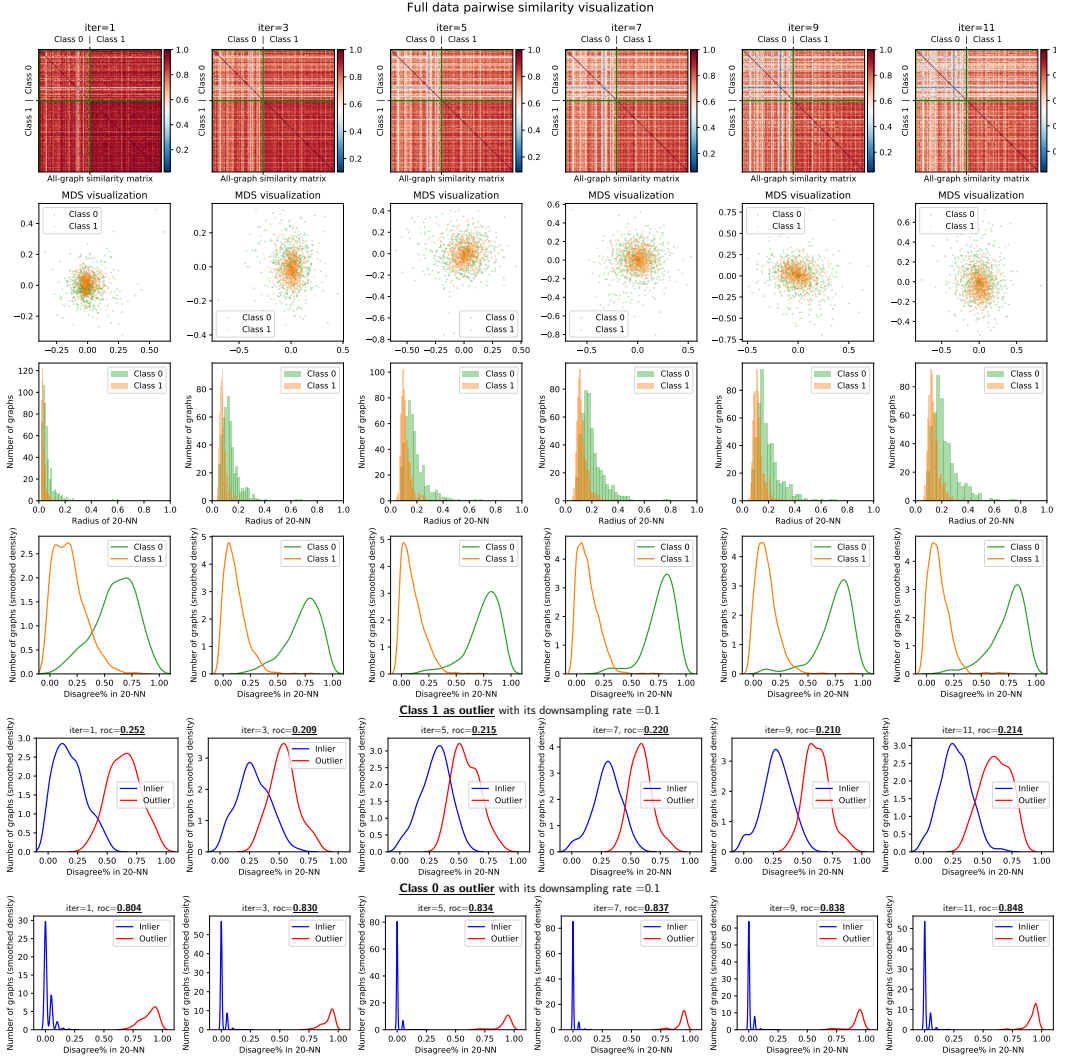
- [27] Guansong Pang, Chunhua Shen, Longbing Cao, and Anton van den Hengel. 2020. Deep Learning for Anomaly Detection: A Review. *CoRR* abs/2007.02500 (2020). <http://dblp.uni-trier.de/db/journals/corr/corr2007.html#abs-2007-02500>
- [28] F. Pedregosa, G. Varoquaux, A. Gramfort, V. Michel, B. Thirion, O. Grisel, M. Blondel, P. Prettenhofer, R. Weiss, V. Dubourg, J. Vanderplas, A. Passos, D. Cournapeau, M. Brucher, M. Perrot, and E. Duchesnay. 2011. Scikit-learn: Machine Learning in Python. *Journal of Machine Learning Research* 12 (2011), 2825–2830.
- [29] Lukas Ruff, Jacob R. Kauffmann, Robert A. Vandermeulen, Grégoire Montavon, Wojciech Samek, Marius Kloft, Thomas G. Dietterich, and Klaus-Robert Müller. 2020. A Unifying Review of Deep and Shallow Anomaly Detection. *CoRR* abs/2009.11732 (2020). <http://dblp.uni-trier.de/db/journals/corr/corr2009.html#abs-2009-11732>
- [30] Lukas Ruff, Robert Vandermeulen, Nico Goernitz, Lucas Deecke, Shoaib Ahmed Siddiqui, Alexander Binder, Emmanuel Müller, and Marius Kloft. 2018. Deep one-class classification. In *International conference on machine learning*. 4393–4402.
- [31] Nino Shervashidze, Pascal Schweitzer, Erik Jan Van Leeuwen, Kurt Mehlhorn, and Karsten M Borgwardt. 2011. Weisfeiler-lehman graph kernels. *Journal of Machine Learning Research* 12, 9 (2011).
- [32] Saurabh Verma and Zhi-Li Zhang. 2017. Hunt for the unique, stable, sparse and fast feature learning on graphs. In *Advances in Neural Information Processing Systems*. 88–98.
- [33] Xuhong Wang, Ying Du, Ping Cui, and Yupu Yang. 2020. OCGNN: One-class Classification with Graph Neural Networks. *arXiv preprint arXiv:2002.09594* (2020).
- [34] B Weisfeiler and A Leman. 1968. The reduction of a graph to canonical form and the algebra which appears therein. *NTI, Series 2* (1968).
- [35] Keyulu Xu, Weihua Hu, Jure Leskovec, and Stefanie Jegelka. 2019. How Powerful are Graph Neural Networks?. In *ICLR*. OpenReview.net. <http://dblp.uni-trier.de/db/conf/iclr/iclr2019.html#XuHLJ19>
- [36] Pinar Yanardag and SVN Vishwanathan. 2015. Deep graph kernels. In *Proceedings of the 21th ACM SIGKDD International Conference on Knowledge Discovery and Data Mining*. 1365–1374.
- [37] Muhan Zhang, Zhicheng Cui, Marion Neumann, and Yixin Chen. 2018. An End-to-End Deep Learning Architecture for Graph Classification.. In *AAAI*, Vol. 18. 4438–4445.
- [38] Xiaojin Zhu and Zoubin Ghahramani. 2002. Learning from Labeled and Unlabeled Data with Label Propagation.

## A APPENDIX

### A.1 Dataset: DD

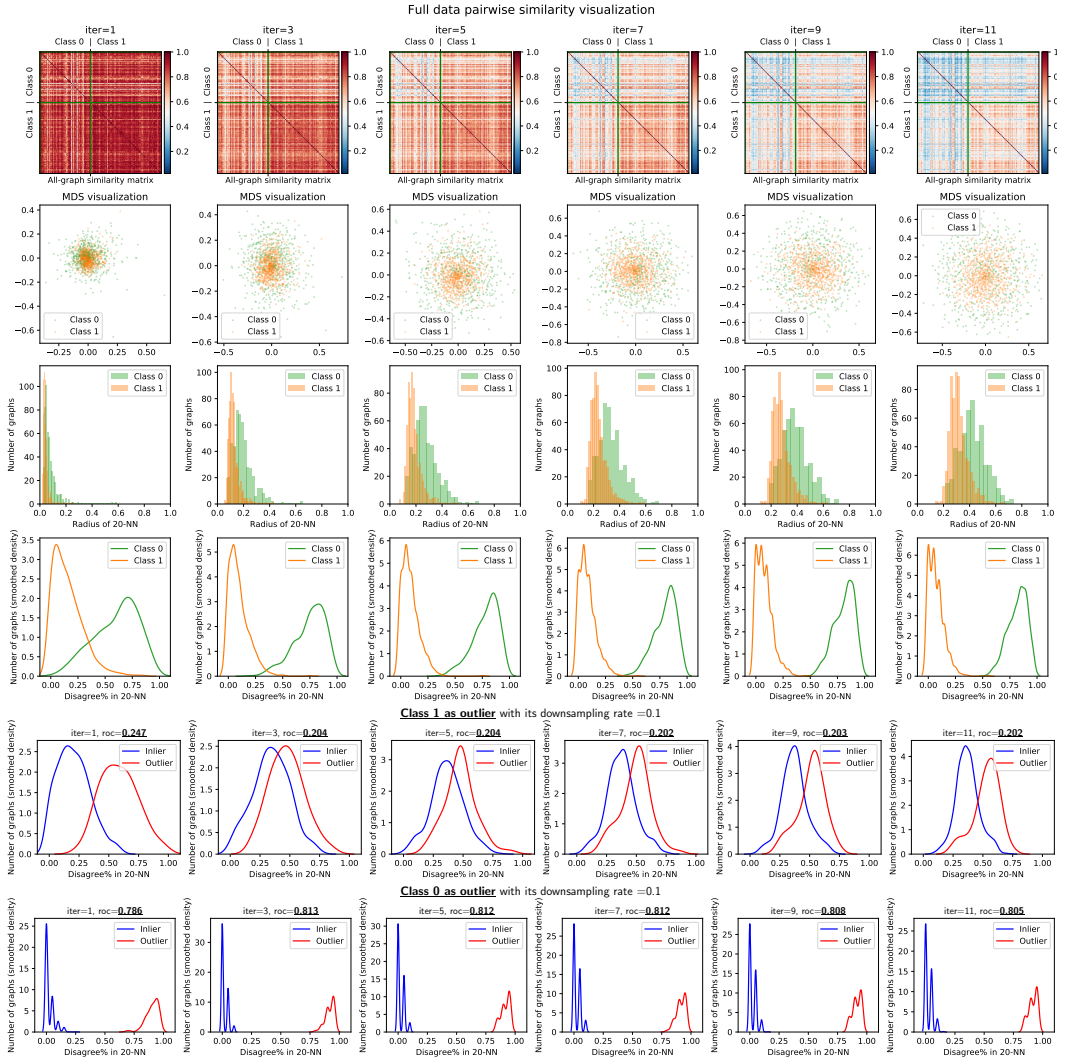
#### A.1.1 PK. Figure 15

Fig. 15. PK+LOF on DD dataset



A.1.2 WL. Figure 16

Fig. 16. WL+LOF on DD dataset



A.1.3 OCGIN. Figure 17

Fig. 17. OCGIN (trained for 25 epochs) on DD dataset

Full data pairwise similarity visualization (trained 25 epochs on downsampled(c=1) dataset)

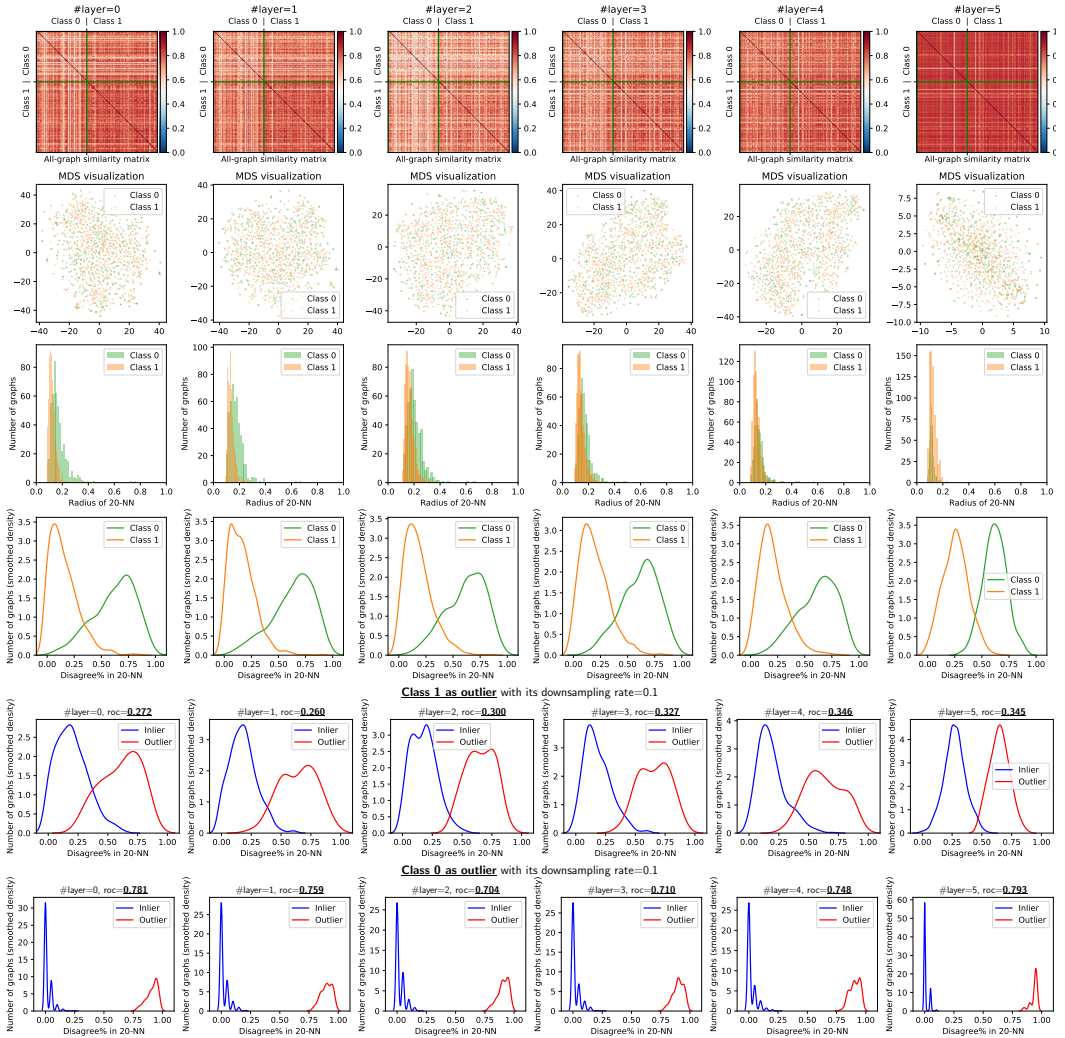


Fig. 18. PK+LOF on DD dataset: effect of (a) number of iterations and (b) down-sampling rate

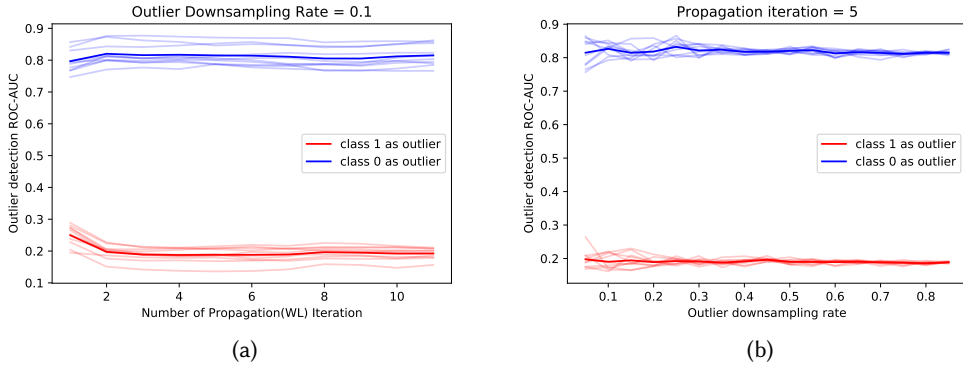


Fig. 19. WL+LOF on DD dataset: effect of (a) number of iterations and (b) down-sampling rate

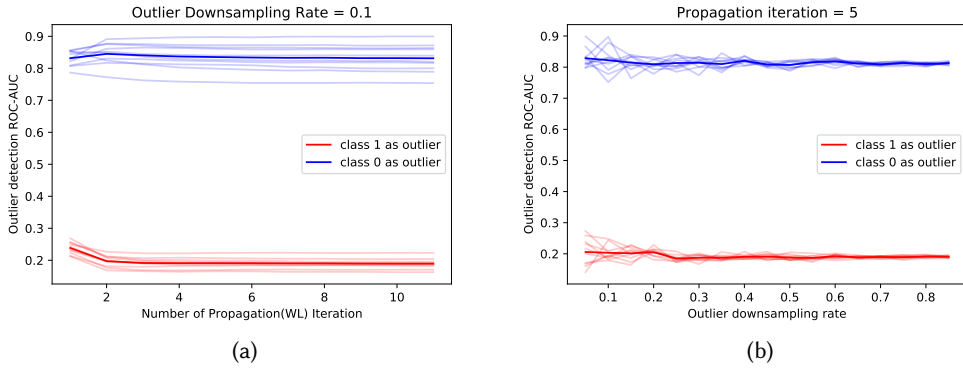
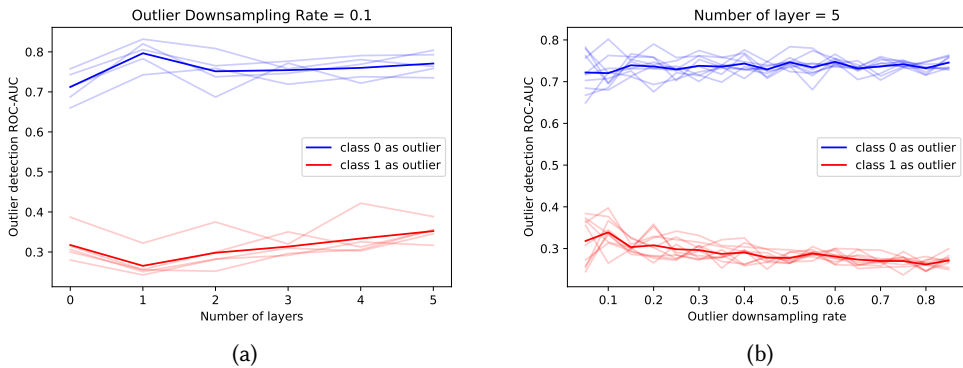


Fig. 20. OCGIN (25 epochs) on DD dataset: effect of (a) number of layers and (b) down-sampling rate rate

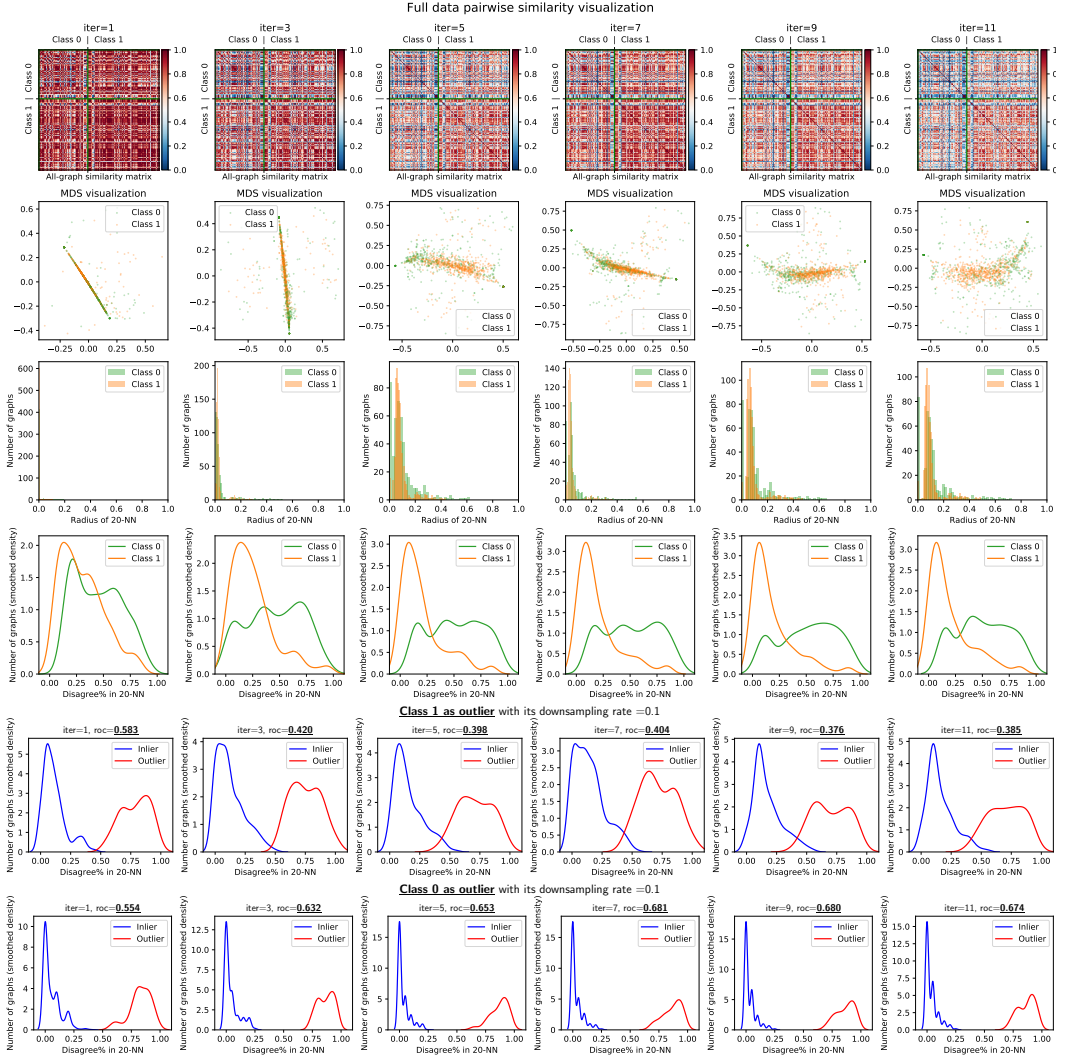


**A.1.4 Performance with increasing graph propagation and varying down-sampling rate.**

## A.2 Dataset: PROTEINS

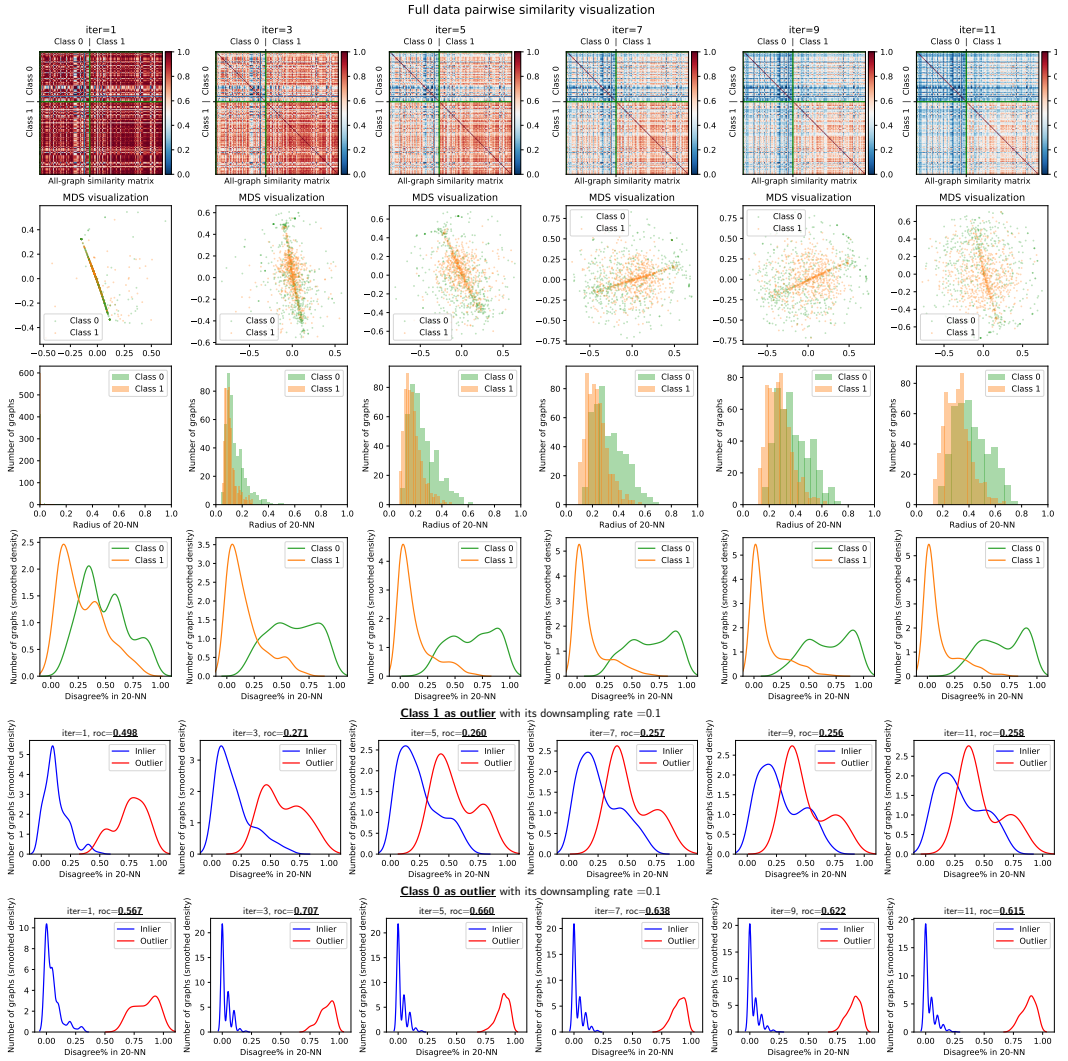
### A.2.1 PK. Figure 21

Fig. 21. PK+LOF on PROTEINS dataset



A.2.2 WL. Figure 22

Fig. 22. WL+LOF on PROTEINS dataset



A.2.3 OCGIN. Figure 23

Fig. 23. OCGIN (25 epochs) on PROTEINS dataset

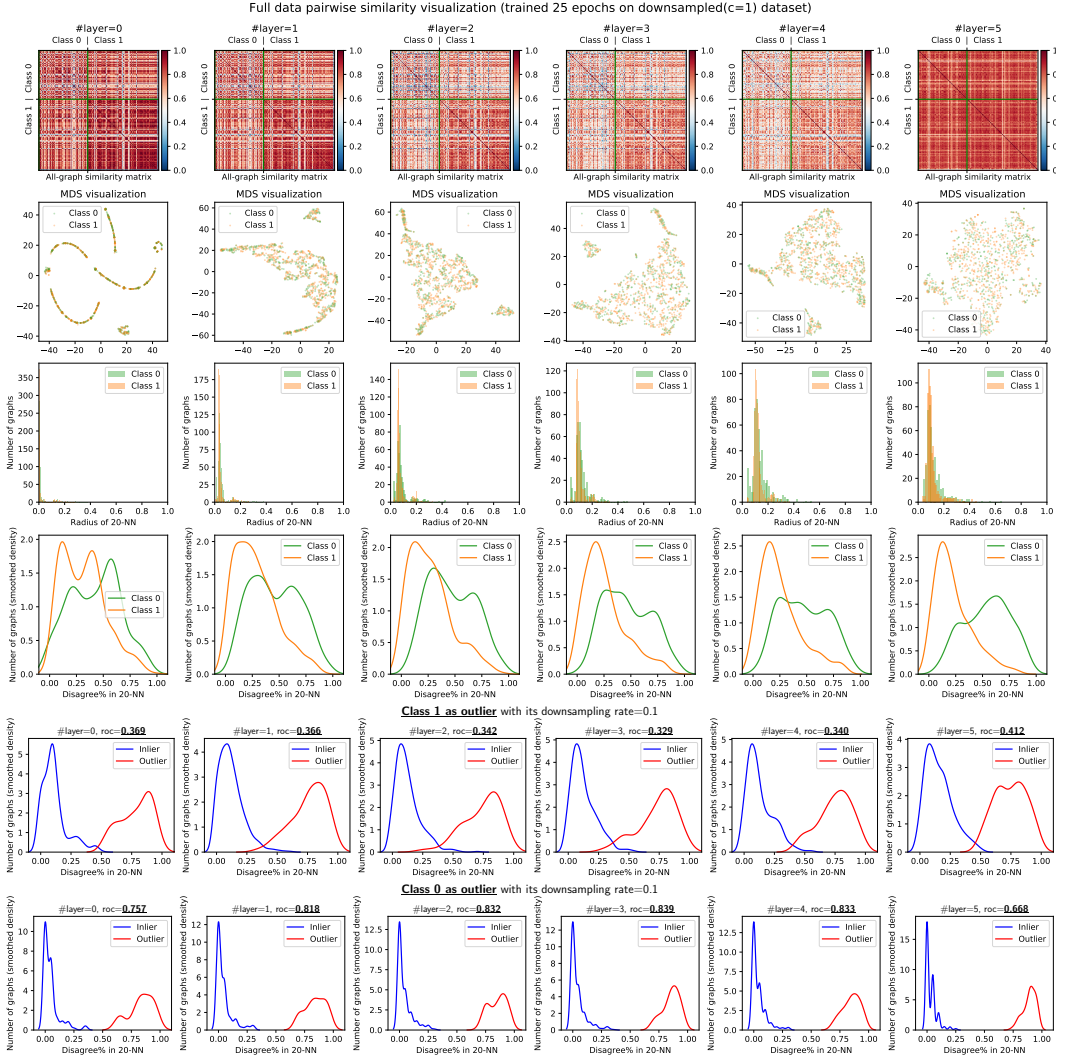


Fig. 24. PK+LOF on PROTEINS dataset: effect of (a) number of iterations and (b) down-sampling rate

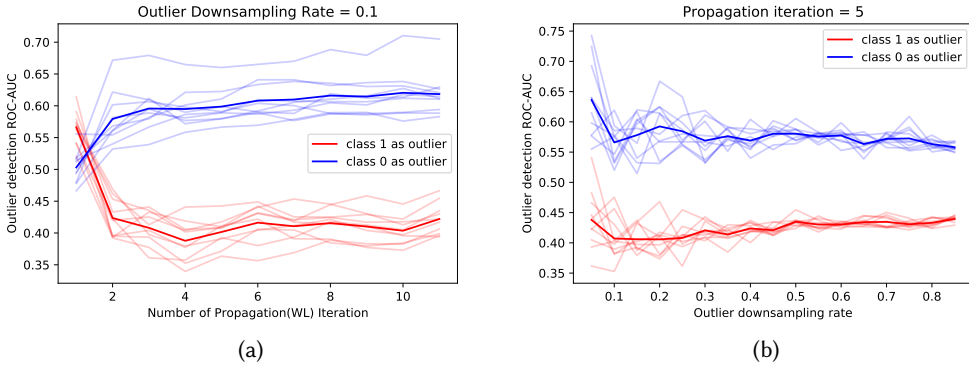


Fig. 25. WL+LOF on PROTEINS dataset: effect of (a) number of iterations and (b) down-sampling rate

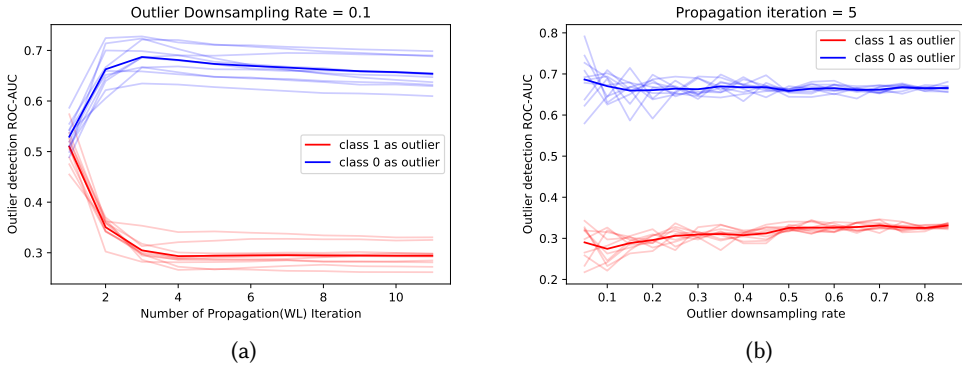
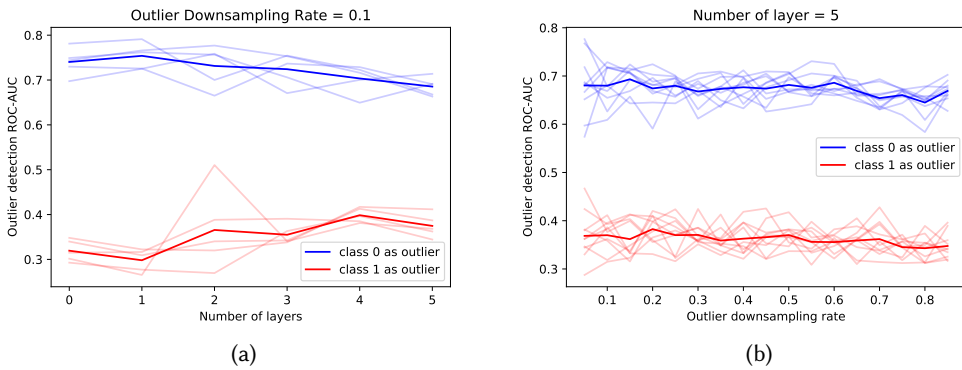


Fig. 26. OCGIN (epoch 25) on PROTEINS dataset: effect of (a) number of layers and (b) down-sampling rate

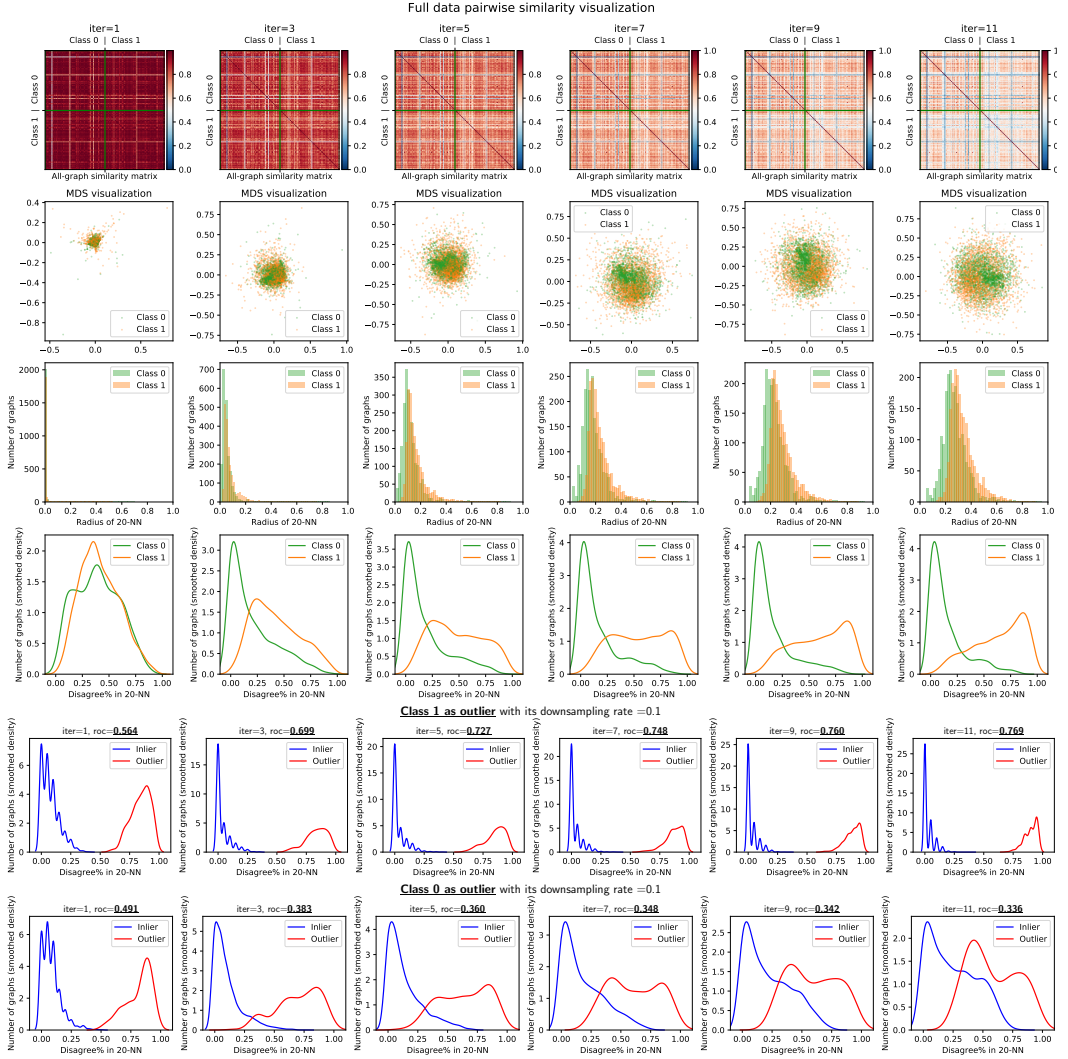


**A.2.4 Performance with increasing graph propagation and varying down-sampling rate.**



A.3.2 WL. Figure 28

Fig. 28. WL+LOF on NCI1 dataset



A.3.3 OCGIN. Figure 29

Fig. 29. OCGIN (25 epochs) on NC11 dataset

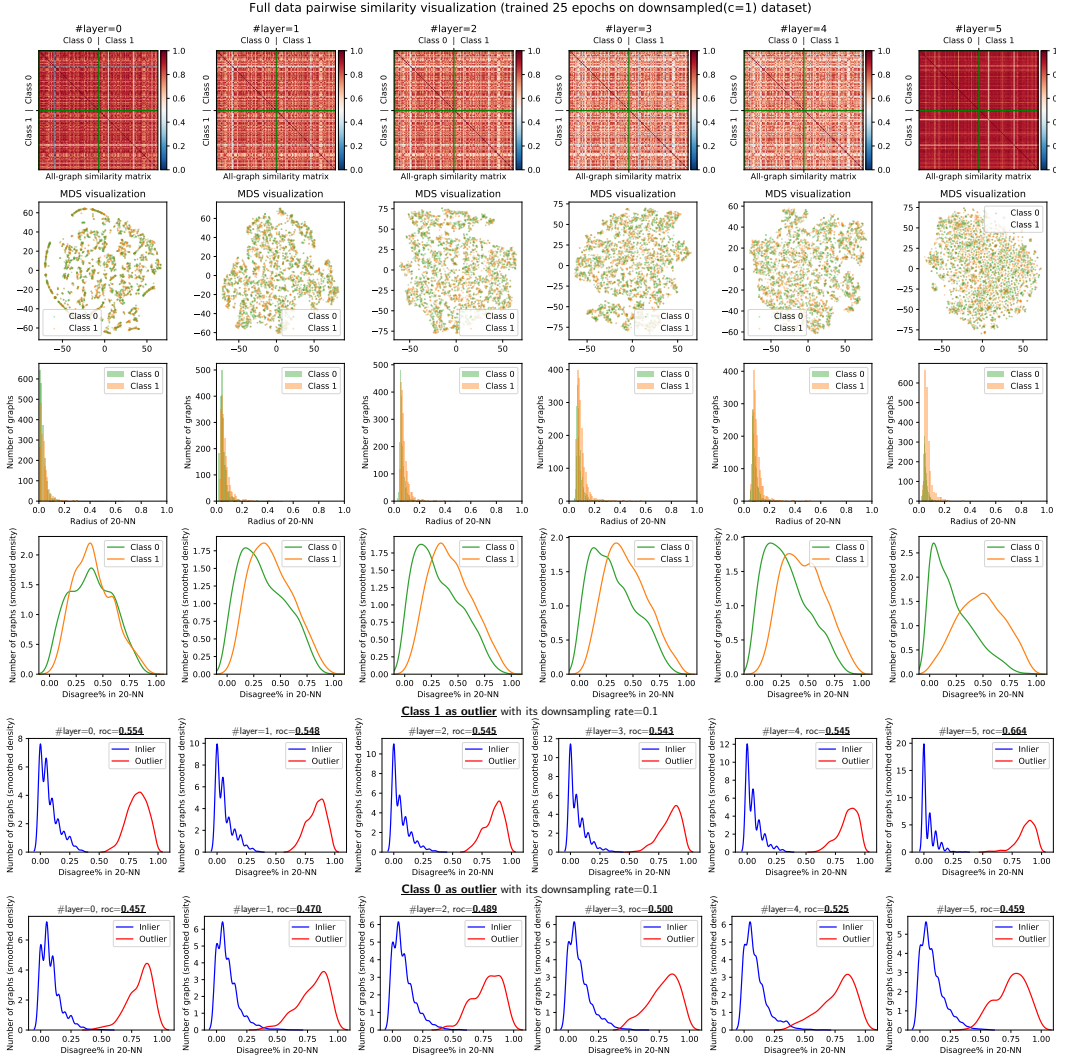


Fig. 30. PK+LOF on NCI1 dataset: effect of (a) number of iterations and (b) down-sampling rate

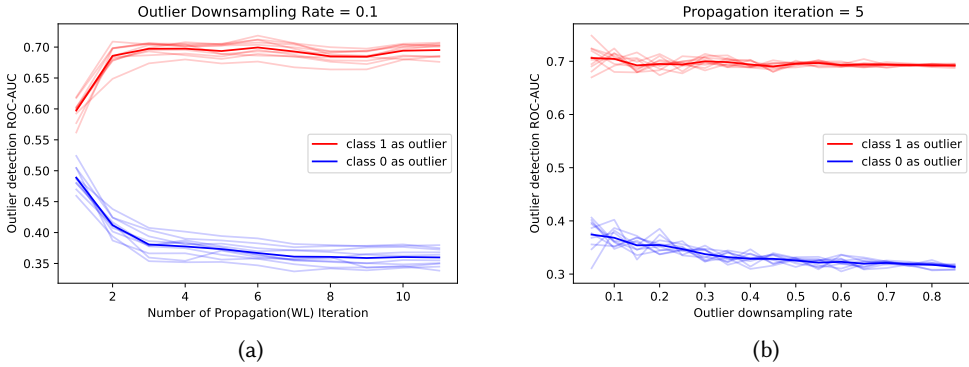


Fig. 31. WL+LOF on NCI1 dataset: effect of (a) number of iterations and (b) down-sampling rate

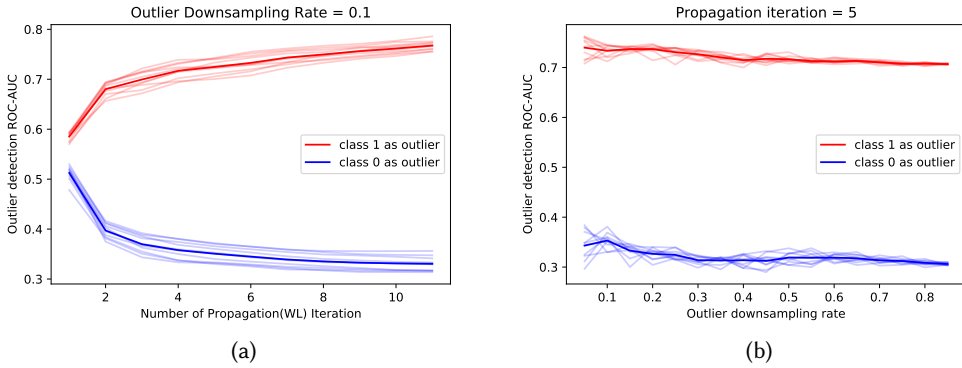
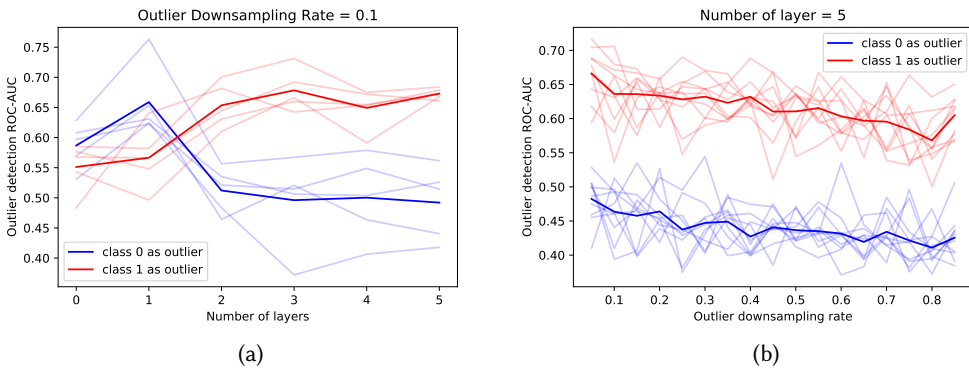


Fig. 32. OCGIN (25 epochs) on NCI1 dataset: effect of (a) number of layers and (b) down-sampling rate

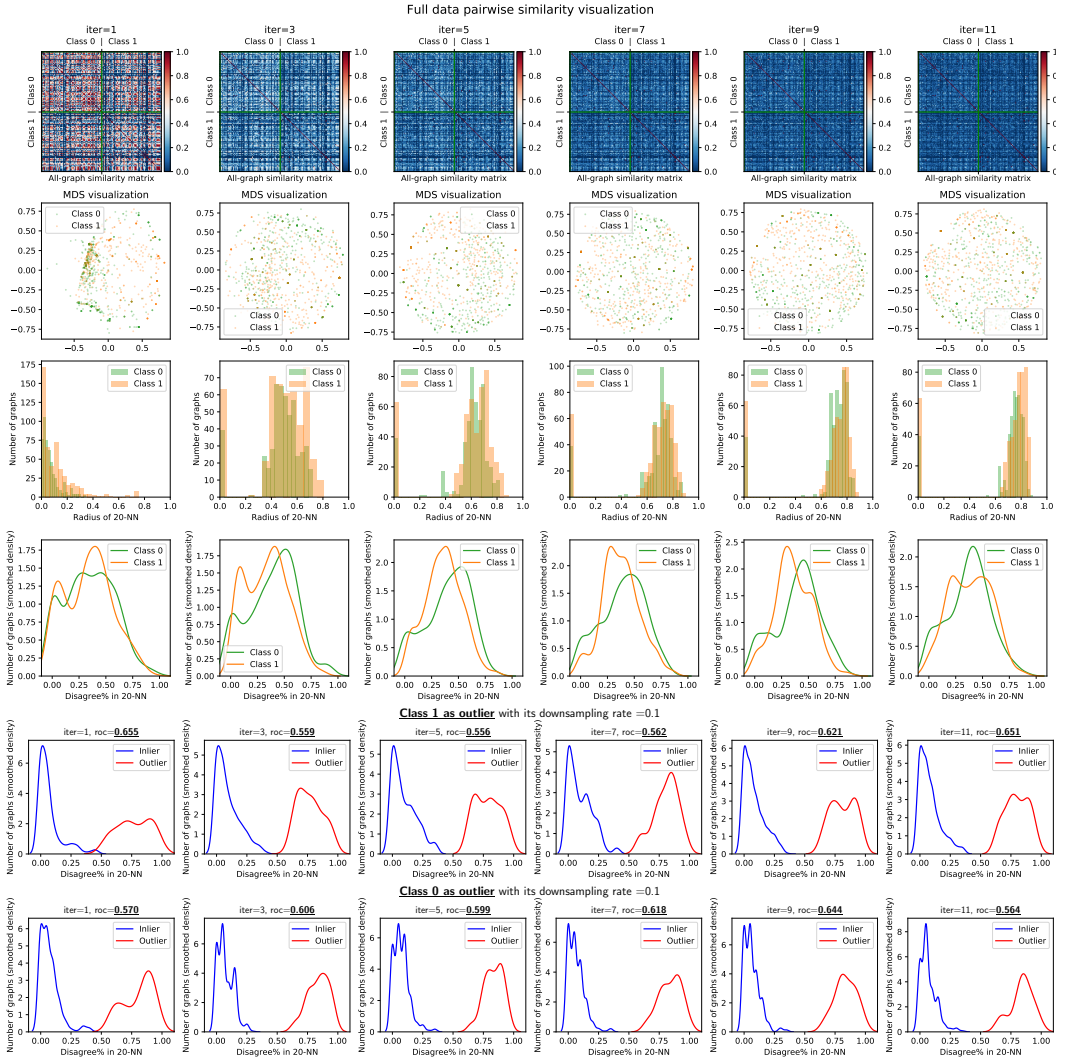


**A.3.4 Performance with increasing graph propagation and varying down-sampling rate.**

## A.4 Dataset: IMDB-BINARY

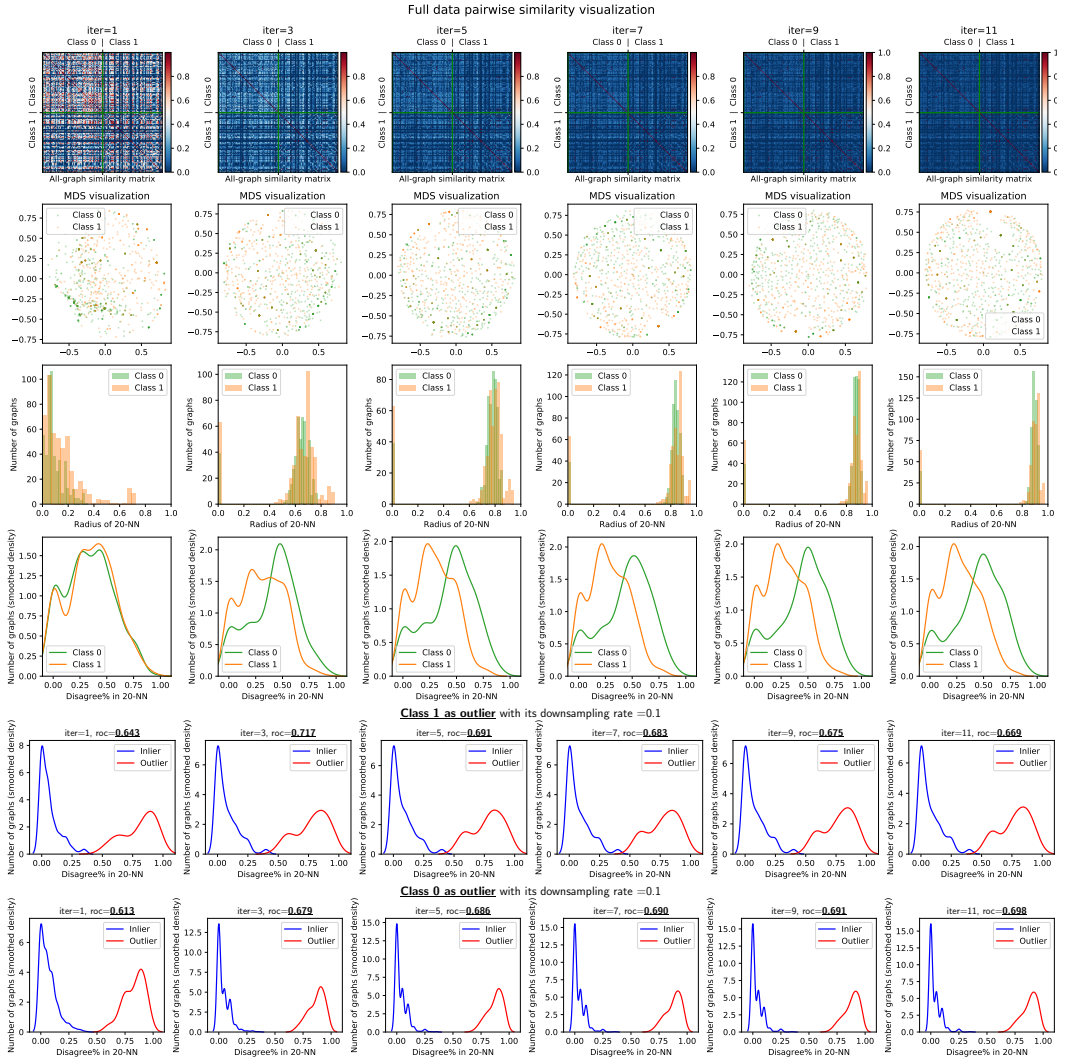
### A.4.1 PK. Figure 33

Fig. 33. PK+LOF on IMDB-BINARY dataset



A.4.2 WL. Figure 34

Fig. 34. WL+LOF on IMDB-BINARY dataset



A.4.3 OCGIN. Figure 35

Fig. 35. OCGIN (25 epochs) on IMDB-BINARY dataset

Full data pairwise similarity visualization (trained 25 epochs on downsampled(c=1) dataset)

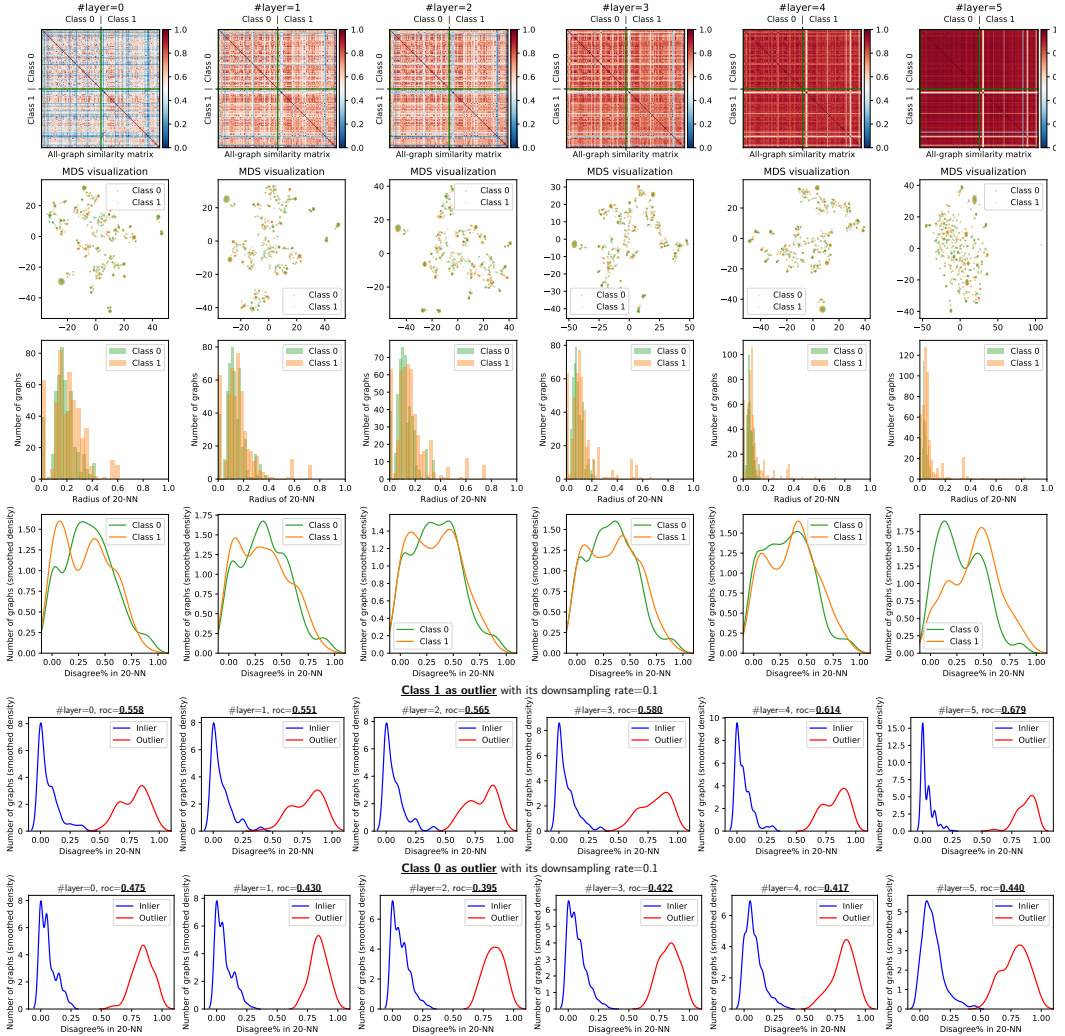


Fig. 36. PK+LOF on IMDB-BINARY dataset: effect of (a) number of iterations and (b) down-sampling rate

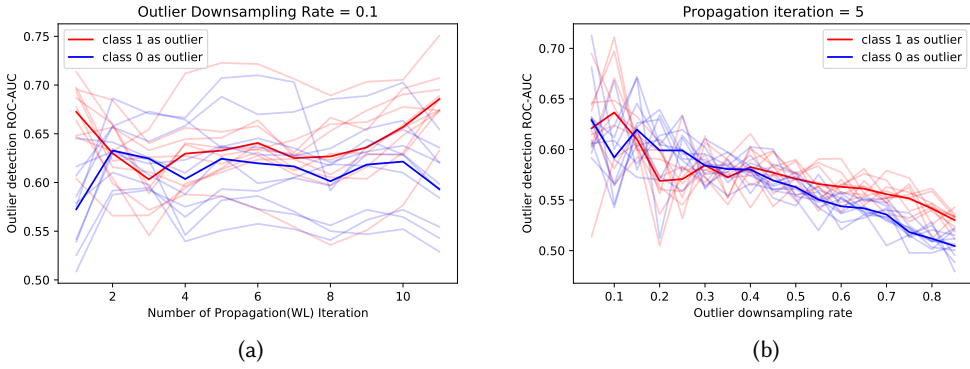


Fig. 37. WL+LOF on IMDB-BINARY dataset: effect of (a) number of iterations and (b) down-sampling rate

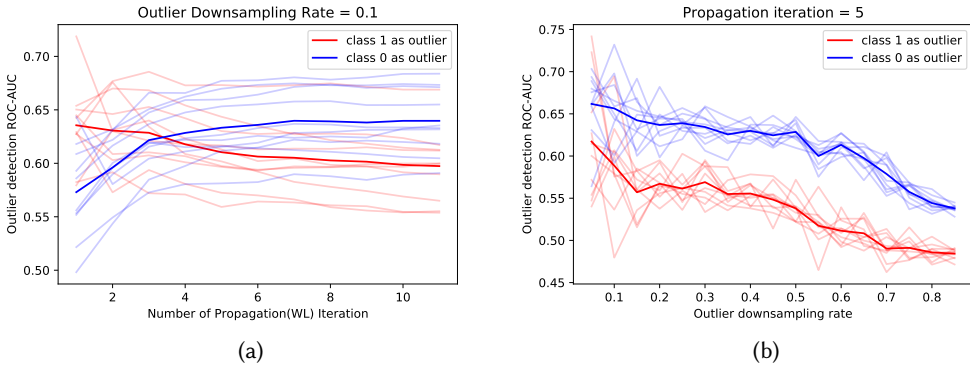
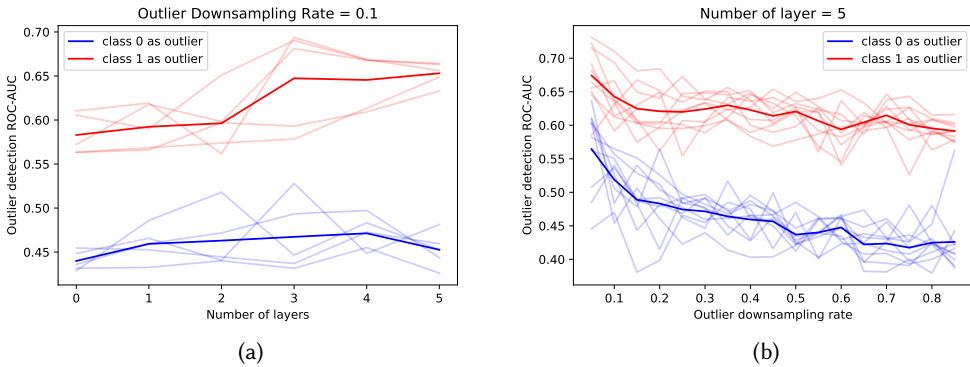


Fig. 38. OCGIN (25 epochs) on IMDB-BINARY dataset: effect of (a) number of layers and (b) down-sampling rate



**A.4.4 Performance with increasing graph propagation and varying down-sampling rate.**